Oncogene

Oncogenic Effects of Evolutionarily Conserved Non-coding RNA *ECONEXIN* on Gliomagenesis

Running title: Evolutionarily conserved lncRNA *ECONEXIN*

Shoichi Deguchi[1,2], Keisuke Katsushima[1], Akira Hatanaka[1], Keiko Shinjo[1], Fumiharu Ohka[2], Toshihiko Wakabayashi[2], Hui Zong[3], Atsushi Natsume[2], and Yutaka Kondo[1]

[1]Department of Epigenomics, Nagoya City University Graduate School of Medical Sciences; [2]Department of Neurosurgery, Nagoya University School of Medicine; [3]University of Virginia School of Medicine

Conflict of interest: The authors disclose no potential conflicts of interest.

*Correspondence to:
Yutaka Kondo, MD, PhD
Department of Epigenomics,
Nagoya City University Graduate School of Medical Sciences
1 Kawasumi, Mizuho-cho, Mizuho-ku,
Nagoya 467-8601, Japan
TEL: +81-52-853-8194, FAX：+81-52-842-3460
E-mail: ykondo@med.nagoya-cu.ac.jp

Abstract

Accumulating studies have demonstrated the importance of long non-coding RNAs (lncRNAs) during oncogenic transformation. However, because most lncRNAs are currently uncharacterized, the identification of novel oncogenic lncRNAs is difficult. Given that intergenic lncRNA have substantially less sequence conservation patterns than protein-coding genes across species, evolutionary conserved intergenic lncRNAs are likely to be functional. The current study identified a novel intergenic lncRNA, *LINC00461* (*ECONEXIN*) using a combined approach consisting of searching lncRNAs by evolutionary conservation and validating their expression in a glioma mouse model. *ECONEXIN* was the most highly conserved intergenic lncRNA containing 83.0% homology with the mouse orthologue (*C130071C03Rik*) for a region over 2,500 bp in length within its exon 3. Expressions of *ECONEXIN* and *C130071C03Rik* were significantly upregulated in both human and mouse glioma tissues. Moreover, the expression of *C130071C03Rik* was upregulated even in pre-cancerous conditions and markedly increased during glioma progression. Functional analysis of *ECONEXIN* in glioma cell lines, U87 and U251, showed it was dominantly located in the cytoplasm and interacted with miR-411-5p via two binding sites within *ECONEXIN*. Inhibition of *ECONEXIN* upregulated miR-411-5p together with the downregulation of its target, Topoisomerase 2 alpha (TOP2A), in glioma cell lines, resulting in decreased cell proliferation. Our data demonstrated that *ECONEXIN* is a potential oncogene that regulates TOP2A by sponging miR-411-5p in glioma. In addition, our investigative approaches to identify conserved lncRNA and their molecular characterization by validation in mouse tumor models may be useful to functionally annotate novel lncRNAs, especially cancer-associated lncRNAs.

Keywords: long non-coding RNA, conservation, glioma

Introduction

Glioma is the most common and lethal brain tumor. Although recent comprehensive molecular profiling in glioma has uncovered several mutations and the aberrant expressions of protein-coding genes, these findings are still insufficient to explain the molecular basis of gliomagenesis[1, 2]. Because the coding genome accounts for less than 2% of all sequences, it is likely that dysregulation of non-coding RNAs might also affect tumor phenotype[3, 4].

Among non-coding RNAs, long non-coding RNAs (lncRNAs) are defined as transcripts >200 nucleotides in length. Recent studies have demonstrated that lncRNAs are involved in multiple biological processes including oncogenic transformation by regulating gene expression. They affect the chromatin structures and RNA interactions, such as those with the microRNA (miRNA) sponge, which upregulates protein expression by inhibiting miRNA binding to their targets[4, 5]. It was reported that lncRNA *HOTAIR* in glioma has an oncogenic role in tumor formation by upregulating FGF1 (Fibroblast growth factor1) by sponging miR-326, which results in activation of the PI3K/AKT and MEK1/2 pathways[6]. In addition, we recently found that Notch1 activation in glioma cells specifically induced the expression of *TUG1*, which coordinately promotes self-renewal by sponging miR-145 in the cytoplasm and recruiting polycomb to repress differentiation genes by the locus-specific methylation of histone H3K27 in the nucleus[7].

Although some lncRNAs share sequences with different protein-coding genes, many lncRNAs are located and transcribed within the intergenic regions that do not overlap exons of protein-coding genes, and are therefore termed intergenic lncRNAs[8-10]. Because evolutionary pressure may differently affect the degree of sequence variation between presumed non-functional regions (e.g. intergenic regions) and functional regions (e.g. protein

coding regions), most intergenic lncRNAs evolve rapidly and show poor sequence conservation[9, 10]. However, recent studies showed that a set of intergenic lncRNAs have a high degree of sequence homology and may have important biological functions across species[9-15]. Indeed, a study of two highly conserved lncRNAs across vertebrates revealed that these lncRNAs have important roles in brain morphogenesis and eye development, which are retained through fishes to mammals[13].

The current study used a pragmatic combination approach of *in silico* analysis focusing on intergenic lncRNA sequence conservation between humans and mice, and the *in vivo* analysis of a glioma mouse model (*Tp53*-/-, *Nf1*-/-)[16]. We identified a novel lncRNA, *LINC00461*, termed evolutionary conserved and expressed in neural tissues (*ECONEXIN*), which has an important role in glioma formation. Our data not only demonstrate a novel axis between lncRNA and miRNA, but also provides information on a novel lncRNA during tumorigenesis.

Results

Identification of a highly conserved lncRNA, *ECONEXIN* (*LINC00461*)

First, we searched for highly conserved intergenic lncRNAs between humans and mice using a public database. The GENCODE catalog (Ver. 21) is one of the most comprehensive databases for non-coding genes with annotations (e.g. gene name, structure, and predicted biological function) in various species. Among the 7,666 human intergenic lncRNAs deposited in GENCODE, only 67 intergenic lncRNAs showed more than 80% sequence homology with mice intergenic lncRNAs in sequences longer than 200 bp (Fig. 1a, Supplementary Table 1, see Materials and Methods)[17].

Among these 67 intergenic lncRNAs, *ECONEXIN* (*LINC00461*, 3,558 bp), was the most highly conserved intergenic lncRNA containing 83.0% homology with the mouse orthologue *C130071C03Rik* in a 2,521bp length within its exon 3 (Fig. 1b, c). *ECONEXIN* was also conserved among other species, including other mammals and birds, suggesting the functional importance of this lncRNA through evolution (Supplementary Fig. 1a). Intriguingly, phylogenetic tree analysis based on the sequences of *ECONEXIN* and its orthologues in each species revealed that evolution of this lncRNA reflects the proposed “timeline of evolutionary history of life” (Supplementary Fig. 1b)[11]. In addition, *ECONEXIN* and *C130071C03Rik* expression was specific to the central nervous system in both humans and mice (Fig. 1d)[18].

Increased expression of *ECONEXIN* in human gliomas

Next, we analyzed the expression of *ECONEXIN* in gliomas, the most malignant central nervous system tumor, by qPCR. *ECONEXIN* expression is upregulated in glioma tissues (n=40) compared to normal brain tissues (n=3) (P<0.001, Fig. 2a, Supplementary Table 2). Two glioma cell lines (U87 and U251) showed a higher expression of *ECONEXIN* compared with a normal neural stem cell line (F3) (P<0.001, Fig. 2b). *ECONEXIN* expression was further examined using a public database TCGA (glioma, n=530; normal, n=4), which showed a significantly higher level of *ECONEXIN* expression in glioma tissues compared to normal brain tissues (P<0.001, Fig. 2c). Intriguingly, lower grade glioma (grade II and III) also showed a significantly high expression level of *ECONEXIN*, suggesting that the dysregulation of *ECONEXIN* is an early event of glioma tumorigenesis (P<0.001, Fig. 2c).

Analysis of *C130071C03Rik* in a glioma mouse model

The use of a tumor-bearing animal model can help understand changes in lncRNA expression during tumor formation. *ECONEXIN* and *C130071C03Rik* are the most highly conserved intergenic lncRNA between humans and mice. Therefore, we examined the contribution of *C130071C03Rik* to glioma tumorigenesis using a spontaneous glioma mouse model, Mosaic Analysis with Double Markers (MADM), which precisely reflects the mosaicism of normal and cancer cells in the brain[16]. In the MADM model, only *Tp53* and *Nf1* homozygous deleted cells express green fluorescent protein (GFP) and these were subsequently transformed into gliomas at post-natal 90-120 days (P90-P120). We examined *C130071C03Rik* expression change in mutant cells (GFP positive cells) from pre-cancerous cells to tumor cells (P20. 60. 90. 120), which were collected by FACS sorting. *C130071C03Rik* expression was significantly increased even in pre-cancerous cells and was significantly increased in P90 and P120 cells (P<0.01), which correspond to tumor cells (Fig. 2d). Although *Tp53* and *Nf1* was homozygously deleted in the GFP positive cells at P6, *C130071C03Rik* expression in the GFP positive cells was comparable with the normal brain tissue cells at the same age (Fig. 2e), indicating that the *C130071C03Rik* expression was not directly regulated by *Tp53* and *Nf1*.

Inhibition of *ECONEXIN* decreases glioma cell proliferation

To examine the effects of *ECONEXIN* in glioma cell proliferation, *ECONEXIN* was depleted in U87 and U251 using five different siRNAs (siRNA#1, #2, #3, #4 and #5), which showed < 50% depletion of *ECONEXIN* expression. Depletion of *ECONEXIN* significantly suppressed glioma cell proliferation (#1–5 in U87, P<0.05; #1–5 in U251, P<0.01; Fig. 1c, 2f, 2g, Supplementary Fig. 2a, 2b). Notably, the miR-9-2 transcript overlapped with the third exon of *ECONEXIN* (Fig. 1c). However, the expression of miR-9-2 was substantially lower compared

to *ECONEXIN* expression and was not affected by siRNA against *ECONEXIN* (Fig. 1c, Fig. 2h, 2i, Supplementary Fig. 2c). These data indicated that the regulation of miR-9-2 expression might be independent of the regulation of *ECONEXIN* expression and that the suppression of proliferation in glioma cell lines by *ECONEXIN* inhibition was independent of the effect of miR-9 activities in this situation.

***ECONEXIN* is dominantly located in cytoplasm and interacts with miR-411-5p**

Next, we examined the subcellular localization of *ECONEXIN* by RNA-FISH analysis. *ECONEXIN* appeared to be dominantly located in the cytoplasm of both U87 and U251 cell lines (Fig. 3a). Almost half of the cells (49.8%) showed the cytoplasmic localization of *ECONEXIN*, while nuclear localization was observed in 23.8% of these cells ($P<0.001$, Fig. 3b).

Cytoplasmic lncRNA sometimes functions as a “sponge”, terminology used to describe the binding of lncRNA to miRNA and repress its inhibitory effect on the target mRNA[19]. To identify potential target miRNAs of the *ECONEXIN* sponge effect, we searched a public database, starBase v2.0. This database is uniquely designed to decode the interactions between different types of RNAs, such as mRNAs, miRNAs, and lncRNAs using large-scale cross-linking immunoprecipitation (CLIP) coupled with sequencing analysis data to avoid potential false positive predictions[20]. Using this database, we found that miR-411-5p was the only miRNA that predictively binds to *ECONEXIN*, which contains two miR-411-5p binding sites (Fig. 1c).

The TCGA database showed that miR-411-5p was significantly downregulated in gliomas (n=526) compared to normal brain tissues (n=5) ($P<0.01$, Fig. 3c). In addition, miR-411-5p expression was significantly inversely correlated with *ECONEXIN* expression ($R=-0.261$,

P<0.001) (Fig. 3d).

Consistent with this expression analysis, the depletion of *ECONEXIN* increased miR-411-5p expression in both U87 and U251 cell lines (Fig. 3e, Supplementary Fig. 3). The relationship between miR-411-5p and *ECONEXIN* expression levels were further examined by RNA-FISH analysis. Although a small number of miR-411-5p signal spots were detected in both U87 and U251 cells, they were significantly increased after *ECONEXIN* inhibition, especially in the cytoplasm (Fig. 3f). Further, we examined miR-411 expression changes in the mutant cells of MADM mouse. In contrast to *C130071C03Rik*, miR-411 expression was significantly downregulated, especially in P90 and P120 cells (*P*<0.01, Fig. 2d, Fig. 3g).

Involvement of *ECONEXIN* and miR-411-5p in RNA-induced silencing complex

The Argonaute protein 2 (AGO2) has a central role in RNA-mediated silencing processes as a catalytic component of the RNA-induced silencing complex (RISC)[21]. To examine whether *ECONEXIN* and miR-411-5p are involved in RNA-mediated silencing, we performed an RNA immunoprecipitation (RIP) assay using antibodies against AGO2 and found that both *ECONEXIN* and miR-411-5p bound to AGO2 in U87 and U251 cells (Fig. 4a). Furthermore, U87 was transfected by expression vectors encoding Flag-AGO2 (WT), Flag-AGO2 mutated PAZ domain (PAZ-mut), or Flag-AGO2 deleted PAZ domain (PAZ-del). FLAG-AGO2 protein expression levels were analyzed by western blotting with anti-FLAG antibody (Fig. 4b). Bindings of *ECONEXIN* and miR-411-5p to AGO2 protein were impaired in mutant forms of AGO2 that had mutated or were devoid of the PAZ domain (Y311A/F312A or complete deletion), which serves as a module for miRNA transfer in RNA silencing and as an anchoring site for the 3' end of guide RNA within silencing effector complexes (Fig. 4c)[7, 22].

ECONEXIN regulates TOP2A by sponging miR-411-5p in gliomagenesis

We analyzed the miR-411-5p targets using starBase V2.0 and identified 700 predicted human genes. These target genes were expected to be upregulated in human gliomas and MADM tumors during tumorigenesis. In fact, microarray analysis showed that among 700 predicted target genes, 305 genes (44%) were upregulated (>1.5) in MADM tumors compared to normal mouse brain tissues. Further, TCGA data showed that among these 305 genes, 120 genes were also significantly upregulated (>1.5) in human glioma compared to normal brain (P<0.05). Among these predicted target genes, topoisomerase 2a (*TOP2A*) showed the highest expression ratio not only in MADM tumors but also in human glioma compared to normal brain. (Fig. 5a, Supplementary Fig 4a, Supplementary Table 3). In addition, *Top2a* was upregulated at early tumorigenesis (P20) (P<0.05, Fig. 5b).

In clinical samples, *TOP2A* showed significantly higher expression in human gliomas compared to normal brains in the TCGA database (glioma n=530, normal n=5, P<0.001, Fig. 5c). *TOP2A* expression was positively correlated with *ECONEXIN* (R=0.204, P<0.001, Fig 5d). Consistently, the depletion of *ECONEXIN* by siRNA repressed TOP2A expression (Fig. 5e, 5f, Supplementary Figure. 4b, 4c). Further, to investigate the potential relationship between *TOP2A*-3' UTR and miR-411-5p, the *TOP2A*-3' UTR, which contained a predictive miR-411-5p target site, was cloned just downstream of the firefly luciferase coding sequence (pmir-*TOP2A*-3' UTR) and transfected into the U87 and U251 cell lines. Significant repression of luciferase activities were observed in both cell lines when precursor molecules mimicking miR-411-5p was transfected (P<0.05, Fig. 5g, Supplementary Fig. 4a).

TOP2A appeared to have an important role in gliomagenesis. Inhibition of TOP2A by siRNA in U87 and U251 cell lines repressed cell growth (Fig. 5h, 5i, 5j). Interestingly, TOP2A overexpression did not significantly affect cell proliferation, indicating that the high expression

of TOP2A is a prerequisite for sustaining continuous tumor cell proliferation but does not promote glioma cell growth (Fig. 5l). The depletion of *ECONEXIN* significantly suppressed cell proliferation, which was rescued by ectopic TOP2A expression (Fig. 2f, Fig. 5k, 5l). These data indicate that TOP2A is an important effector to maintain glioma cell proliferation, which is regulated by *ECONEXIN*-miR-411-5p interactions via a sponge function during gliomagenesis (Fig. 5k, 5l).

Discussion

Although dysregulation of the non-coding genome derives important cancer phenotypes, most of the lncRNAs involved are currently uncharacterized. Deciphering the physiological roles of cancer-associated lncRNAs needs a transition in investigative approaches from lncRNA annotation and molecular characterization to tumorigenic mouse models[4, 23]. In the current study, we used a public database to identify 67 intergenic lncRNAs that are highly conserved with more than 80% sequence homology between humans and mice in sequences longer than 200 bp. This criterion was also used to identify the conserved lncRNA, Tcl1 upstream neuron-associated (*TUNA*), which shows remarkable sequence conservation beyond species and which has a vital role in the pluripotency and neural differentiation of embryonic stem cells[17]. Intriguingly, the 67 identified lncRNAs contained *MIAT*, *KANTR*, *TUNA*, *MEG3*, and *MALAT1*, whose functions were reported to also be associated with neuronal development and function[17, 23-26], suggesting that this strategy for the identification of functional lncRNAs is effective and that evolutionally conserved lncRNAs sometimes have important roles in neural differentiation as was reported previously (Supplementary Table 1)[12].

We found that *ECONEXIN* was the most highly conserved among the 67 identified lncRNAs. Expression analysis of the *ECONEXIN* orthologue, *C130071C03Rik*, in a glioma

mouse model, showed that the dysregulation of *C130071C03Rik* occurred in early glioma tumorigenesis. Orthologous lncRNAs generally show similar cell type specific expression and stage specific regulation during embryonic development. Indeed, a previous study showed that human islet lncRNAs and mouse orthologous transcripts were regulated in a similar manner and that dysregulation of these lncRNAs was closely associated with type 2 diabetes[27]. These data suggest that the integrated analysis of conservation-based transcriptomes coupled with an experimental mouse model may be an effective strategy to identify the potential roles of lncRNAs.

ECONEXIN/C130071C03Rik expression appears not to be directly regulated by *Tp53* and *Nf1*. Intriguingly, *ECONEXIN* and *C130071C03Rik* showed more than 80% sequence homology in their promoter region (~500 bp upstream of transcriptional start site). Transcriptional factor binding motif analysis using the JASPAR database revealed that 140 transcription factors may bind to the *ECONEXIN* and *C130071C03Rik* promoter regions[28]. Among the 140 predicted transcription factors, we identified 13 transcription factors, of which expression levels were higher in both human gliomas and mouse gliomas than in normal brain tissues. These transcription factors included SOX3 and TCF12, which have been known to be involved in neural development and glioma formation as well[29 30] (Supplementary Table 4). Therefore, it may be plausible that these transcription factors are involved in the regulation of *ECONEXIN* and *C130071C03Rik* expression.

It was considered that at least more than twice the number of lncRNAs are located in the cytoplasm compared to the nucleus[31]. Some lncRNAs in the cytoplasm act as miRNA sponges, by binding to miRNAs to quench their activity, resulting in the regulation of protein expression[4, 7].

It might be unlikely that *ECONEXIN* has only one target miRNA (i.e. miR-411-5p). Indeed,

using public database, miRWALK 2.0[32], we found 51 miRNAs, which have possible miRNA binding sites within both *ECONEXIN* and *C130071C03Rik* sequences. Interestingly, among these 51 miRNA, expression of 42 miRNAs (82.4%) including miR-411-5p was significantly inversely correlated with *ECONEXIN* expression in gliomas (n=526) in TCGA database, suggesting that *ECONEXIN* may function as multiple miRNA sponge during glioma formation. However, in the current study, we identified miR-411-5p as an *ECONEXIN* target using more empirical database, Starbase v2.0, which is based on large-scale CLIP coupled with sequencing analysis data to avoid potential false positive predictions [20] and focused on the functional analysis of this miRNA during glioma formation.

ECONEXIN is dominantly located in the cytoplasm, and contains two miR-411-5p binding sites. We discovered that both *ECONEXIN* and miR-411-5p bound to AGO2 protein, a component of RISC, indicating that *ECONEXIN* is involved in the regulation of miRNA via RISC machinery. It was also proposed that the amount of cytoplasmic lncRNA should be at least more than the amount of miRNA to demonstrate miRNA sponge function[33]. We found that cytoplasmic *ECONEXIN* expression was more abundant compared to miR-411-5p in glioma cells, while *ECONEXIN* depleted cells showed significantly increased levels of miR-411-5p. Thus, *ECONEXIN* modulates miR-411-5p levels through its function as a miRNA sponge to trap miR-411-5p, which results in TOP2A upregulation during glioma formation.

ECONEXIN-miR-411-5p-TOP2A axis appears to play an important role in early glioma tumorigenesis. *TOP2A* encodes DNA topoisomerase II alpha (TOP2A), an enzyme that controls DNA topologic states during DNA replication[34]. Our data indicated that the overexpression of TOP2A is required for the maintenance of aggressive tumor cell proliferation, but its expression is not sufficient to promote tumor cell growth. Consistent with our findings, the overexpression of TOP2A was associated with an advanced stage,

aggressive tumor phenotype, and poor prognosis in various types of cancers[35]. Based on this evidence, a DNA topoisomerase 2 inhibitor, etoposide, is widely used for the treatment of many types of cancers including glioma[35, 36]. However, etoposide treatment sometimes causes severe adverse effects such as myelosuppression and secondary malignancies, which may be partly caused by the inhibition of DNA replication by etoposide in hematopoietic cells with proliferative activity[37, 38]. In the current study, we showed that the inhibition of *ECONEXIN* effectively decreased TOP2A expression. Because *ECONEXIN* is specifically expressed in neural tissues, but not in blood cells, TOP2A suppression by the inhibition of *ECONEXIN* may reduce the myelosuppressive side effects observed for systemic etoposide treatments. Taken together, the current study demonstrated a novel mechanism, in which the *ECONEXIN*-miR-411-5p-TOP2A axis is an essential contributor to the acquired malignant phenotype in glioma, which may be a potential therapeutic target for glioma treatment.

Recent accumulating studies of glioma have reported a wide variety of mechanisms involved in gliomagenesis. Here, we identified a novel lncRNA associated pathway in the formation of glioma. Targeting lncRNA or its function in cancer cells provides a novel strategy for cancer therapy, because certain lncRNAs are gene specific and/or tissue epigenetic regulators[4, 39]. Developing RNA-targeting therapeutics may be a promising option to modulate lncRNAs for anti-cancer treatments. Regarding targeting lncRNAs methods, antisense oligonucleotides (ASO) might also be a potent treatment option. ASO are chimeric RNA/DNA oligonucleotides that direct RNase H to cleave target lncRNA and deplete the transcripts regardless of their cellular localization[4, 7, 40]. Using this type of treatment might provide more effective therapeutic options for glioma with fewer side-effects. In conclusion, our results highlight the importance of the lncRNA derived miR-411-5p-TOP2A axis in glioma formation and provide a strong rationale for targeting *ECONEXIN* as a specific and potent

therapeutic approach to treat gliomas.

Materials and Methods

Glioma tissues and cell line samples

Forty glioma tissue samples were obtained from patients undergoing surgical treatment at Nagoya University Hospital, Japan. Written informed consent was received from all patients. A diagnosis of glioma was determined histologically by experienced pathologists. The backgrounds of the patients are shown in Supplementary Table 2. Human U87 and U251 glioma cell lines were obtained from American Type Culture Collection (ATCC, Manassas, VA, USA). Although these cell lines were not authenticated, relatively low passage number cells were obtained. F3, a human neural stem cell (NSC) line, was established as described previously[41]. All cell lines were maintained in DMEM medium (Thermo Fisher Scientific, Waltham, MA, USA) containing 10% fetal bovine serum (Thermo Fisher Scientific) and 1% penicillin-streptomycin (Thermo Fisher Scientific) at 37°C in a humidified incubator with 5% CO_2.

Glioma mouse model and cell sorting of GFP positive cells

The MADM glioma mouse model, which is used to analyze aberrations in individual cell lineages prior to final transformation, was established and examined according to a previous study[16, 42]. In this model, mutant cells with the homozygous deletion of *Tp53* and *Nf1* genes via Cre/loxP-mediated mitotic inter-chromosomal recombination show a green color by GFP expression, while their sibling wild type cells show a red color by red fluorescent protein (RFP). Only green colored cells spontaneously developed glioma at post-natal 90-120 days.

GFP-positive mutant cells were collected at P20, P60, P90, and P120 by sorting cells using a FACS ARIA II (BD Bioscience, San Jose, CA, USA). All experiments were conducted under protocols approved by the Institutional Animal Care and Use Committee of Nagoya City University Graduate School of Medical Sciences.

RNA extraction and quantitative reverse transcription-polymerase chain reaction (qRT-PCR)

Total RNA was extracted from tissues and cells with TRIzol reagent (Thermo Fisher Scientific). Total RNA from normal brain tissues (n=3) was purchased from BioChain (Cat # R1234043-10, Lot # B501146; Cat # R1234042-10, Lot # B810027; Cat # R1234051-50, Lot # B604039, Hayward, CA, USA). RNA was reverse-transcribed with Prime Script RT Master Mix (Takara, Kusatsu, Japan) or a TaqMan MicroRNA RT Kit (Thermo Fisher Scientific) according to the manufacturer' s instructions. TaqMan PCR and SYBR Green quantitative PCR (qPCR) were carried out in triplicate for the target genes. Expression levels of target genes were determined using the delta-delta Ct (cycle threshold) method, and normalized to *GAPDH*. Expression levels of target microRNAs were normalized to RNU6B (human) or snoRNA 202 (mouse). Oligonucleotide primers for TaqMan PCR assays (Thermo Fisher Scientific) and primer sets for SYBR Green assays are shown in Supplementary Table 5.

Western blot analysis

Cell lysates were extracted from U87 and U251 cells. Fifty μg of each protein was run on 10% SDS/PAGE gels, transferred to nitrocellulose membranes, and incubated with the following antibodies as primary antibodies: rabbit polyclonal anti-TOP2A (ab12318; Abcam, Cambridge, UK), mouse monoclonal anti-FLAG (F1804; Sigma-Aldrich, St. Louis, MO, USA),

and mouse monoclonal anti-β-actin (#3700; Cell Signaling Technology, Danvers, MA). HRP-linked anti-mouse IgG (#7076, Cell Signaling Technology) and HRP-linked anti-rabbit IgG (#7074, Cell Signaling Technology) antibodies were used as secondary antibodies.

Microarray analysis

RNA from mouse tissues was amplified into cRNA and labeled according to the Agilent One-Color Microarray-Based Gene Expression Analysis protocol (Agilent Technologies, Santa Clara, CA). Labeled samples were purified with the RNeasy Kit (Qiagen, Valencia, CA, USA) and hybridized to SurePrint G3 Mouse GE 8 x 60K array slides (G4858A, Agilent Technologies) at 65°C with rotation at 10 rpm for 17 hours. The arrays were scanned using an Agilent Microarray Scanner (G2565BA, Agilent Technologies). The scanned images were analyzed using the Feature Extraction software, version 10.7.3.1 (Agilent Technologies) with background correction. Data analysis was performed with GeneSpring GX, version 12.6.0 (Silicon Genetics, Redwood City, CA, USA). Microarray analysis was performed in duplicate for wild type mice and in triplicate for the MADM model. The data from our microarrays are available in ArrayExpress (http://www.ebi.ac.uk/arrayexpress; Accession code: GSE91050).

RNA interference

To inhibit gene expression, U87 and U251 were transfected with 50 nM specific gene siRNA or control non-targeting siRNA (Silencer Select Negative Control #1 siRNA, 4390844, Thermo Fisher Scientific) using Lipofectamine 3000 (Thermo Fisher Scientific). Forty-eight hours after the transfection of siRNA, total RNA was extracted from U87 or U251 cell lines, and the effects were validated by qRT-PCR. siRNA sequences are shown in Supplementary Table 6.

Cell proliferation assay

U87 and U251 cells at a density of 2.5 x 10^3 cells per well were cultured in 96-well plates for 24 hours in normal conditions before treatments. Cell proliferation was assessed every 24 hours using a Cell Counting Kit 8 (Dojindo, Kumamoto, Japan) according to the manufacturer's instructions.

RNA Fluorescence in situ hybridization

RNA Fluorescence in situ hybridization (RNA-FISH) was performed using the QuantiGene ViewRNA ISH Cell Assay (Affymetrix, Frederick, MD, USA). Briefly, tissue sections were rehydrated and incubated with proteinase K. Subsequently, they were incubated with ViewRNA probe sets designed against human *LINC00461 (ECONEXIN)* (VA1-18109-06, Affymetrix) and miR-411-5p (VM1-99999-01, Affymetrix).

RNA binding protein immunoprecipitation assay

RIP assay was performed using RiboCluster Profiler RIP-Assay Kit (RN1005, MBL International, Watertown, MA) [7]. RNA-protein complexes were immunoprecipitated with anti-AGO2 antibody (RN005M, MBL International), anti-Flag antibody (F1804, Sigma-Aldrich), and anti-IgG antibody as a negative control (PM035, MBL International). Immunoprecipitated RNA was analyzed by qRT-PCR. To examine the interaction between RNA and the AGO2 PAZ domain, U87 cells were transfected with expression vectors encoding either Flag-AGO2, Flag-AGO2 with mutated PAZ domain (Y311A/F312A) or Flag-AGO2 with complete deletion of PAZ domain. The details of the AGO2 vectors mutated PAZ domain were described previously[7]. Primer sequences for construction of FLAG-AGO2 variant vector were shown in

Supplementary Table 7.

Dual-Luciferase Reporter Assay

The fragments of the *TOP2A*-3' UTR region were amplified by PCR with the primers which were shown in Supplementary Table 8. The fragments of *TOP2A*-3' UTR were then ligated into the XbaI and XhoI site of the pmirGLO luciferase reporter vector (Promega,Madison,WI). For the reporter assay, luciferase constructs (100 ng) were co-transfected into the cells using Lipofectamine 3000 (Thermo Fisher Scientific) with 50nM precursor molecules mimicking miR-411-5p (ID: MC11409) (Thermo Fisher Scientific) or Pre-miR miRNA precursor negative control #1 (Thermo Fisher Scientific). Luciferase activity was measured 48 hours after transfection using a Dual-Luciferase reporter assay system (Promega). To obtain the relative luciferase activity, firefly luminescence was normalized by the Renilla luminescence.

Construction of the TOP2A expression vector

The *TOP2A* gene was amplified by PCR using KOD-plus-neo (TOYOBO, Osaka, Japan). The primer sequences are shown in Supplementary Table 8. The amplified DNA fragment was cloned into pENTR/D-TOPO vector (Thermo Fisher Scientific), followed by transferring into a Gateway pcDNA-DEST47 Vector using Gateway cloning technology (Thermo Fisher Scientific). The vector sequences were validated by conventional sequencing analysis. Transfection of DNA vectors was performed using Lipofectamine 3000 according to the manufacturer's instructions (Thermo Fisher Scientific).

Identification of highly conserved intergenic lncRNAs

Using GENCODE gene annotation, lncRNAs were classified by their location with respect to

the protein coding gene. A subtype “intergenic lncRNA, lincRNA” was defined as transcripts that are intergenic noncoding RNA loci with a length > 200 bp. Specifically, this type of lncRNA does not intersect with any protein coding loci. The boundaries of the protein coding loci were defined as 5 kb upstream of the start codon and 30 kb downstream from the stop codon[43]. We downloaded the human and murine intergenic lncRNA sequences from GENCODE 21 and GENCODE M4（http://www.gencodegenes.org/), respectively. Then, we analyzed the sequence homologies of intergenic lncRNAs between humans and mice by using the Basic Local Alignment Search Tool (BLAST) website at the National Center for Biotechnology (NCBI)（http://blast.ncbi.nlm.nih.gov/Blast.cgi). We sorted human intergenic lncRNAs with highly conserved regions (more than 80% sequence homology with mouse sequences longer than 200 bp). We also sorted murine intergenic lncRNAs with highly conserved regions. Finally, by overlapping each result, we identified highly conserved intergenic lncRNAs between humans and mice.

Database and phylogenetic analysis

To analyze gene expression (*ECONEXIN,* hsa-miR-411-5p and *TOP2A*) in clinical glioma samples, we used the level-3 preprocessed expression data of RNA-seq (IlluminaHiseq) from The Cancer Genome Atlas (TCGA) (https://tcga-data.nci.nih.gov/). Phylogenetic trees were constructed using MEGA 6.0 software[44] with the neighbor joining method. The RNA sequences in each species, which are orthologues of *LINC00461*, were obtained from the BLAST database.

Statistics

The statistical significance of differences between two groups was analyzed by the paired Student's t-test. All reported *P* values were two-sided, and $P<0.05$ was considered statistically significant.

Acknowledgements :

This study was performed as research programs of the Project for Development of Innovative Research on Cancer Therapeutics (P-Direct), Ministry of Education, Culture, Sports, Science and Technology of Japan (Y. Kondo), of the PRESTO, JST (Y. Kondo), and of the Grant-in-Aid for Scientific Research, the Japan Society for the Promotion of Science (25290048, Y. Kondo).

References

1 Suzuki H, Aoki K, Chiba K, Sato Y, Shiozawa Y, Shiraishi Y *et al* (2015). Mutational landscape and clonal architecture in grade II and III gliomas. *Nat Genet* 47: 458-468.

2 Ceccarelli M, Barthel FP, Malta TM, Sabedot TS, Salama SR, Murray BA *et al* (2016). Molecular Profiling Reveals Biologically Discrete Subsets and Pathways of Progression in Diffuse Glioma. *Cell* 164: 550-563.

3 Wahlestedt C (2013). Targeting long non-coding RNA to therapeutically upregulate gene expression. *Nat Rev Drug Discov* 12: 433-446.

4 Schmitt AM, Chang HY (2016). Long Noncoding RNAs in Cancer Pathways. *Cancer Cell* 29: 452-463.

5 Guttman M, Donaghey J, Carey BW, Garber M, Grenier JK, Munson G *et al* (2011). lincRNAs act in the circuitry controlling pluripotency and differentiation. *Nature* 477: 295-300.

6 Ke J, Yao YL, Zheng J, Wang P, Liu YH, Ma J *et al* (2015). Knockdown of long non-coding RNA HOTAIR inhibits malignant biological behaviors of human glioma cells via modulation of miR-326. *Oncotarget* 6: 21934-21949.

7 Katsushima K, Natsume A, Ohka F, Shinjo K, Hatanaka A, Ichimura N *et al* (2016). Targeting the Notch-regulated non-coding RNA TUG1 for glioma treatment. *Nature communications* 7: 13616.

8 Kapranov P, Willingham AT, Gingeras TR (2007). Genome-wide transcription and the implications for genomic organization. *Nat Rev Genet* 8: 413-423.

9 Guttman M, Amit I, Garber M, French C, Lin MF, Feldser D *et al* (2009). Chromatin signature reveals over a thousand highly conserved large non-coding RNAs in mammals. *Nature* 458: 223-227.

10 Quinn JJ, Zhang QC, Georgiev P, Ilik IA, Akhtar A, Chang HY (2016). Rapid evolutionary turnover underlies conserved lncRNA-genome interactions. *Genes Dev* 30: 191-207.

11 Washietl S, Kellis M, Garber M (2014). Evolutionary dynamics and tissue specificity of human long noncoding RNAs in six mammals. *Genome Res* 24: 616-628.

12 Hezroni H, Koppstein D, Schwartz MG, Avrutin A, Bartel DP, Ulitsky I (2015). Principles of long noncoding RNA evolution derived from direct comparison of transcriptomes in 17 species. *Cell Rep* 11: 1110-1122.

13 Ulitsky I, Shkumatava A, Jan CH, Sive H, Bartel DP (2011). Conserved function of lincRNAs in vertebrate embryonic development despite rapid sequence evolution.

Cell 147: 1537-1550.

14 Kutter C, Watt S, Stefflova K, Wilson MD, Goncalves A, Ponting CP *et al* (2012). Rapid turnover of long noncoding RNAs and the evolution of gene expression. *PLoS Genet* 8: e1002841.

15 Cabili MN, Trapnell C, Goff L, Koziol M, Tazon-Vega B, Regev A *et al* (2011). Integrative annotation of human large intergenic noncoding RNAs reveals global properties and specific subclasses. *Genes Dev* 25: 1915-1927.

16 Liu C, Sage JC, Miller MR, Verhaak RG, Hippenmeyer S, Vogel H *et al* (2011). Mosaic analysis with double markers reveals tumor cell of origin in glioma. *Cell* 146: 209-221.

17 Lin N, Chang KY, Li Z, Gates K, Rana ZA, Dang J *et al* (2014). An evolutionarily conserved long noncoding RNA TUNA controls pluripotency and neural lineage commitment. *Mol Cell* 53: 1005-1019.

18 Oliver PL, Chodroff RA, Gosal A, Edwards B, Cheung AF, Gomez-Rodriguez J *et al* (2015). Disruption of Visc-2, a Brain-Expressed Conserved Long Noncoding RNA, Does Not Elicit an Overt Anatomical or Behavioral Phenotype. *Cerebral cortex (New York, NY : 1991)* 25: 3572-3585.

19 Tay Y, Rinn J, Pandolfi PP (2014). The multilayered complexity of ceRNA crosstalk and competition. *Nature* 505: 344-352.

20 Li JH, Liu S, Zhou H, Qu LH, Yang JH (2014). starBase v2.0: decoding miRNA-ceRNA, miRNA-ncRNA and protein-RNA interaction networks from large-scale CLIP-Seq data. *Nucleic Acids Res* 42: D92-97.

21 Carthew RW, Sontheimer EJ (2009). Origins and Mechanisms of miRNAs and siRNAs. *Cell* 136: 642-655.

22 Ma JB, Ye K, Patel DJ (2004). Structural basis for overhang-specific small interfering RNA recognition by the PAZ domain. *Nature* 429: 318-322.

23 Sauvageau M, Goff LA, Lodato S, Bonev B, Groff AF, Gerhardinger C *et al* (2013). Multiple knockout mouse models reveal lincRNAs are required for life and brain development. *eLife* 2: e01749.

24 Sone M, Hayashi T, Tarui H, Agata K, Takeichi M, Nakagawa S (2007). The mRNA-like noncoding RNA Gomafu constitutes a novel nuclear domain in a subset of neurons. *J Cell Sci* 120: 2498-2506.

25 Mo CF, Wu FC, Tai KY, Chang WC, Chang KW, Kuo HC *et al* (2015). Loss of non-coding RNA expression from the DLK1-DIO3 imprinted locus correlates with reduced neural differentiation potential in human embryonic stem cell lines. *Stem cell research & therapy* 6: 1.

26 Bernard D, Prasanth KV, Tripathi V, Colasse S, Nakamura T, Xuan Z *et al* (2010). A long nuclear-retained non-coding RNA regulates synaptogenesis by modulating gene expression. *EMBO J* 29: 3082-3093.

27 Moran I, Akerman I, van de Bunt M, Xie R, Benazra M, Nammo T *et al* (2012). Human beta cell transcriptome analysis uncovers lncRNAs that are tissue-specific, dynamically regulated, and abnormally expressed in type 2 diabetes. *Cell metabolism* 16: 435-448.

28 Mathelier A, Fornes O, Arenillas DJ, Chen CY, Denay G, Lee J *et al* (2016). JASPAR 2016: a major expansion and update of the open-access database of transcription factor binding profiles. *Nucleic Acids Res* 44: D110-115.

29 Holmberg J, He X, Peredo I, Orrego A, Hesselager G, Ericsson C *et al* (2011). Activation of neural and pluripotent stem cell signatures correlates with increased malignancy in human glioma. *PLoS ONE* 6: e18454.

30 Labreche K, Simeonova I, Kamoun A, Gleize V, Chubb D, Letouze E *et al* (2015). TCF12 is mutated in anaplastic oligodendroglioma. *Nature communications* 6: 7207.

31 Ulitsky I (2016). Evolution to the rescue: using comparative genomics to understand long non-coding RNAs. *Nat Rev Genet* 17: 601-614.

32 Dweep H, Gretz N (2015). miRWalk2.0: a comprehensive atlas of microRNA-target interactions. *Nat Methods* 12: 697.

33 Denzler R, Agarwal V, Stefano J, Bartel DP, Stoffel M (2014). Assessing the ceRNA hypothesis with quantitative measurements of miRNA and target abundance. *Mol Cell* 54: 766-776.

34 Pommier Y, Leo E, Zhang H, Marchand C (2010). DNA topoisomerases and their poisoning by anticancer and antibacterial drugs. *Chemistry & biology* 17: 421-433.

35 Chen T, Sun Y, Ji P, Kopetz S, Zhang W (2015). Topoisomerase IIalpha in chromosome instability and personalized cancer therapy. *Oncogene* 34: 4019-4031.

36 Leonard A, Wolff JE (2013). Etoposide improves survival in high-grade glioma: a meta-analysis. *Anticancer Res* 33: 3307-3315.

37 Clark PI, Slevin ML, Joel SP, Osborne RJ, Talbot DI, Johnson PW *et al* (1994). A randomized trial of two etoposide schedules in small-cell lung cancer: the influence of pharmacokinetics on efficacy and toxicity. *J Clin Oncol* 12: 1427-1435.

38 Mistry AR, Felix CA, Whitmarsh RJ, Mason A, Reiter A, Cassinat B *et al* (2005). DNA topoisomerase II in therapy-related acute promyelocytic leukemia. *N Engl J Med* 352: 1529-1538.

39 Yang G, Lu X, Yuan L (2014). LncRNA: a link between RNA and cancer. *Biochimica*

et biophysica acta 1839: 1097-1109.

40 Ideue T, Hino K, Kitao S, Yokoi T, Hirose T (2009). Efficient oligonucleotide-mediated degradation of nuclear noncoding RNAs in mammalian cultured cells. *RNA (New York, NY)* 15: 1578-1587.

41 Kim SU (2004). Human neural stem cells genetically modified for brain repair in neurological disorders. *Neuropathology* 24: 159-171.

42 Zong H, Espinosa JS, Su HH, Muzumdar MD, Luo L (2005). Mosaic analysis with double markers in mice. *Cell* 121: 479-492.

43 Derrien T, Johnson R, Bussotti G, Tanzer A, Djebali S, Tilgner H *et al* (2012). The GENCODE v7 catalog of human long noncoding RNAs: analysis of their gene structure, evolution, and expression. *Genome Res* 22: 1775-1789.

44 Tamura K, Stecher G, Peterson D, Filipski A, Kumar S (2013). MEGA6: Molecular Evolutionary Genetics Analysis version 6.0. *Molecular biology and evolution* 30: 2725-2729.

Figure legends

Figure 1. Identification of a highly conserved intergenic lncRNA, *LINC00461, ECONEXIN*. (a) Pipeline for the identification of highly conserved intergenic lncRNAs between humans and mice. Annotations of intergenic lncRNAs were obtained from the GENCODE database. (b) Length of the conserved region (homology >80% between humans and mice, X-axis) of 67 highly conserved intergenic lncRNAs. (c) Upper panel shows a schematic diagram of the *LINC00461* (*ECONEXIN*) gene locus as annotated on the UCSC Genome Browser. Pre-miR-9-2 (horizontal stripes) is overlapped with the third exon of *LINC00461*. Lower panel shows the transcribed RNA of *LINC00461*. Black allow heads show siRNA target sites against *LINC00461* (#1-5) used in this study. Gray allows show predicted binding sites of miR-411-5p in *LINC00461*. (d) Expression level of *ECONEXIN* in 53 different human tissues. Analyzed data were obtained from GTEx (Genotype Tissue Expression) (version V6p, http://www.gtexportal.org/home/). X-axis indicates tissue names. The examined numbers of samples are shown after tissue names in parentheses. Y-axis indicates the median RPKM (Reads per kilobase of transcript per million mapped reads) value.

Figure 2. Inhibition of *ECONEXIN* (si-*ECONEXIN* #1-3) decreases glioma cell proliferation. (a) Expression levels of *ECONEXIN* in clinical normal brain (cerebral cortex, n=3) and glioma (n=40) samples were examined by qRT-PCR. Bars indicate median. ***, $P<0.001$. (b) Expression levels of *ECONEXIN* in normal neural stem cell (F3) and glioma cell lines (U87 and U251). Y-axis indicates expression level relative to F3 (log_2). Experiments were performed in triplicate. Error bars indicate S.D (standard deviation). ***, $P<0.001$.

(c) Expression levels of *ECONEXIN* in clinical normal brain (n=4), lower grade glioma (LGG,

n=530), and glioblastoma (GBM, n=151) samples are presented as a box-whisker plot. Data were obtained from the TCGA database. Middle horizontal line inside box indicates the median. Bottom and top of the box indicates the 25th and 75th percentiles, respectively. The ends of the whiskers indicate the minimum and maximum of all of the data, respectively. Y-axis indicates expression levels of *ECONEXIN* by RPKM value +1 (log_2). ***, *P*<0.001 (d) Expression levels of *C130071C03Rik* in normal brain (gray bars) and glioma cells (black bars) in MADM mice. X-axis indicates post-natal days. Y-axis indicates expression level normalized to *Gapdh*. Experiments were performed in triplicate. Error bars indicate S.D. *, *P*<0.05, **, *P*<0.01, ***, *P*<0.001. (e) Expression levels of *C130071C03Rik* in normal brain tissues (gray bar) and pre-cancerous GFP positive cells (*Tp53*-/-, *Nf1*-/-; black bar) in MADM mice at postnatal 6 days. Y-axis indicates expression level normalized to *Gapdh*. Experiments were performed in triplicate. N.S, not significant. (f) Expression levels of *ECONEXIN* in U87 (left) and U251 (right) cells treated with si-negative control (si-*NC*), si-*ECONEXIN* #1, #2 or #3. Y-axis indicates expression level relative to si-*NC*. Experiments were performed in triplicate. Error bars indicate S.D. *, *P*<0.05. (g) Effects of si-*ECONEXIN* #1, #2 and #3 on proliferation of U87 (left) and U251 cells (right). X-axis indicates time after each siRNA treatment. Y-axis indicates cell number relative to si-*NC.* Experiments were performed in triplicate. Error bars indicate S.D. *, *P*<0.05, **, *P*<0.01. (h) Expression levels of *ECONEXIN* and miR-9-2 in U87 (left) and U251 cells (right). Y-axis indicates expression level relative to *ECONEXIN*. Experiments were performed in triplicate. Error bars indicate S.D. *, *P*<0.05, **, *P*<0.01. (i) Expression levels of miR-9-2 in U87 (left) and U251 cells (right) treated with si-*NC,* si- *ECONEXIN* #1, #2 or #3. Y-axis indicates expression level relative to *si-NC*. Experiments were performed in triplicate. Error bars indicate S.D (n=3). N.S, not significant

Figure 3. Predominant location of *ECONEXIN* in cytoplasm. (a) Left panel shows the RNA-FISH analysis of *ECONEXIN* (red) in U87 (left) and U251 cells (right). Nuclei are stained with DAPI. Bars: 10 μm. Right graph shows the spot numbers related to *ECONEXIN* detection per cell in U87 and U251 cells. Error bars indicate S.D (n=10). (b) Three patterns of subcellular localization of *ECONEXIN* in U251 cells (left). Type 1 and 3 show dominant *ECONEXIN* localization in either the nucleus or cytoplasm, respectively. Type 2 shows comparable localization of *ECONEXIN* in the nucleus and cytoplasm. Numbers of the three types of cells were calculated per 100 cells (right). Cell counting was performed four times. Bar indicates the median. **, $P<0.01$. (c) Expression levels of miR-411-5p in clinical normal brain and glioma samples are presented as a box-whisker plot. Data were obtained from TCGA data sets. Middle horizontal line inside box indicates the median. Bottom and top of the box indicates the 25th and 75th percentiles, respectively. The ends of the whiskers indicate the minimum and maximum of all of the data, respectively. Y-axis indicates expression levels of miR-411-5p by RPM (reads per million) miRNA mapped values (log_2) in either normal brain (n=5) or glioma tissues (n=526). **, $P<0.01$. (d) Relationship of expression levels between *ECONEXIN* and miR-411-5p in glioma samples (n=526) from the TCGA database. X-axis indicates expression levels of *ECONEXIN*. Y-axis indicates expression levels of miR-411-5p. *P* values were obtained by Pearson's correlation coefficient analysis. The red line in the graph indicates linear approximation ($R=-0.261$). (e) Expression levels of miR-411-5p in U87 and U251 cells treated with si-*NC,* si-*ECONEXIN* #1, #2 or #3. Y-axis indicates expression level relative to siRNA-negative control (si-*NC*). Experiments were performed in triplicate. Error bars indicate S.D. *, $P<0.05$. (f) Left panel shows RNA-FISH analysis of miR-411-5p (red) in U87 (upper) and U251 cells (lower) treated with si-*NC* (left)

or si-*ECONEXIN* (right). Nuclei are stained with DAPI. Bars: 10 μm. Right graph shows spot numbers related to miR-411-5p detection per cell in U87 (left) and U251 (right) cells treated with either si-*NC* or si-*ECONEXIN*. Error bars indicate S.D (n=3). ***, *P*<0.001. (g) Expression levels of mmu-miR-411 in normal brain (gray bars) and glioma cells (black bars) in MADM mice. X-axis indicates post-natal days. Y-axis indicates expression level normalized to *snoRNA202*. Experiments were performed in triplicate. Error bars indicate S.D. *, *P*<0.05, **, *P*<0.01, ***, *P*<0.001.

Figure 4. Involvement of *ECONEXIN* and miR-411-5p in RISC. (a) RIP analysis of *ECONEXIN* and miR-411-5p in U87 (left) and U251 cells (right) was performed using an antibody against AGO2 or IgG as a negative control. Enrichment of *ECONEXIN* and miR-411-5p are expressed as a percentage of input RNA. Y-axis indicates normalized fold enrichment to IgG. Experiments were performed in triplicate. Error bars indicate S.D. ***, *P*<0.001. (b) Schematic diagram shows construction of the FLAG-AGO2 vector. The PAZ domain was mutated as Y311A/F312A (PAZ-mut) or completely deleted (229-347, PAZ-del) (upper). FLAG-AGO2 protein expression levels were analyzed by western blotting with anti-FLAG antibody in U87 cells. WT, wild type FLAG-AGO2. β-actin protein expression was used as an internal control. (Lower) (c) RIP analysis of *ECONEXIN* and miR-411-5p was performed using an antibody against Flag (black bar) or IgG (gray bar) as a negative control. Enrichment of *ECONEXIN* and miR-411-5p is expressed as a percentage of input RNA. Y-axis indicates normalized fold enrichment to IgG. Experiments were performed in triplicate. Error bars indicate S.D. **, *P*<0.01, ***, *P*<0.001.

Figure 5. *ECONEXIN* regulates DNA replication by sponging miR-411-5p in

gliomagenesis. (a) Schematic diagram to identify the target of miR-411-5p. Human miR-411-5p target genes were predicted by starBase V2.0. Among the 700 genes, *Top2a* showed the highest expression ratio between both human glioma tissues and normal brain tissues, and MADM glioma cells and normal mouse brain cells. (b) Expression levels of *Top2a* in normal mouse brain cells (gray bars) and tumor cells in MADM (black bars). X-axis indicates post-natal days. Y-axis indicates expression level relative to *Gapdh*. Experiments were performed in triplicate. Error bars indicate S.D (n=3). **, $P<0.01$, ***, $P<0.001$. (c) Expression levels of *TOP2A* in clinical normal brain and glioma samples are presented as a box-whisker plot. Data were obtained from TCGA data sets. Middle horizontal line inside box indicates the median. Bottom and top of the box indicates the 25th and 75th percentiles, respectively. The ends of the whiskers indicate the minimum and maximum of all of the data, respectively. Y-axis indicates expression levels of *TOP2A* by RSEM (RNA-Seq by Expectation-Maximization) value plus 1 (log_2) in normal brain (n=5) and glioma (n=530) tissues. ***, $P<0.001$. (d) Relationship between the expression levels of *ECONEXIN* and *TOP2A* in glioma samples (n=530) from the TCGA database. X-axis and Y-axis indicate expression levels of *ECONEXIN* and *TOP2A*, respectively. Data were analyzed by Pearson's correlation coefficient analysis. The red line in the graph indicates linear approximation (R=0.204). (e) Expression level of *TOP2A* in U87 (left) and U251 cells (right) treated with si-*NC,* si-*ECONEXIN* #1, #2 or #3. Y-axis indicates expression level relative to siRNA-negative control (si-*NC*). Experiments were performed in triplicate. Error bars indicate S.D. *, $P<0.05$, **, $P<0.01$. (f) Protein expression levels of TOP2A in U87 (left) and U251 cells (right) treated with si-*NC,* si-*ECONEXIN* #1, #2 or #3. (g) Dual-Luciferase assay with the pmir-*TOP2A*-3' UTR reporter vector in U87 and U251 cells. Cells were co-transfected with 50nM precursor molecules pre-miR-411-5p (Pre-411-5p) or negative control miRNA

precursor (Pre-NC). Y-axis indicates relative luciferase activity to pmir-emp control (i.e. reporter vector without *TOP2A*-3' UTR sequence). The assays were performed in triplicate. Error bars indicate S.D. *, *P*<0.05, **, *P*<0.01. (h) Expression levels of *TOP2A* in U87 and U251 cells treated with si-*NC* or si-*TOP2A*. Y-axis indicates expression level relative to si-*NC*. Experiments were performed in triplicate. Error bars indicate S.D. **, *P*<0.01, P<0.001. (i) Protein expression levels of TOP2A in U87 and U251 cells treated with si-*NC* or si-*TOP2A.* (j) Effects of si-*TOP2A* on the proliferation of U87 and U251 cells. X-axis indicates time after treatment of si-RNA against each target. Y-axis indicates cell number relative to si-*NC.* Experiments were performed in triplicate. Error bars indicate S.D (n=3). *, *P*<0.05, **, *P*<0.01, ***, *P*<0.001. (k) U87 and U251 cells were transfected with si-*NC* or si-*ECONEXIN* and with empty vector or expression vectors encoding *TOP2A*. Protein expression levels of TOP2A in U87 (left) and U251 cells (right) after 72 hours of transfection were analyzed by western blotting with anti-TOP2A antibody. β-actin was used as an internal control. (l) Effects of ectopic TOP2A expression on cell proliferation in *ECONEXIN* depleted U87 (left) and U251 (right) cells. X-axis indicates time after each treatment. Y-axis indicates cell number relative to si-*NC* plus empty vector. Experiments were performed in triplicate. Error bars indicate S.D. ***, *P*<0.001.

Figure 1

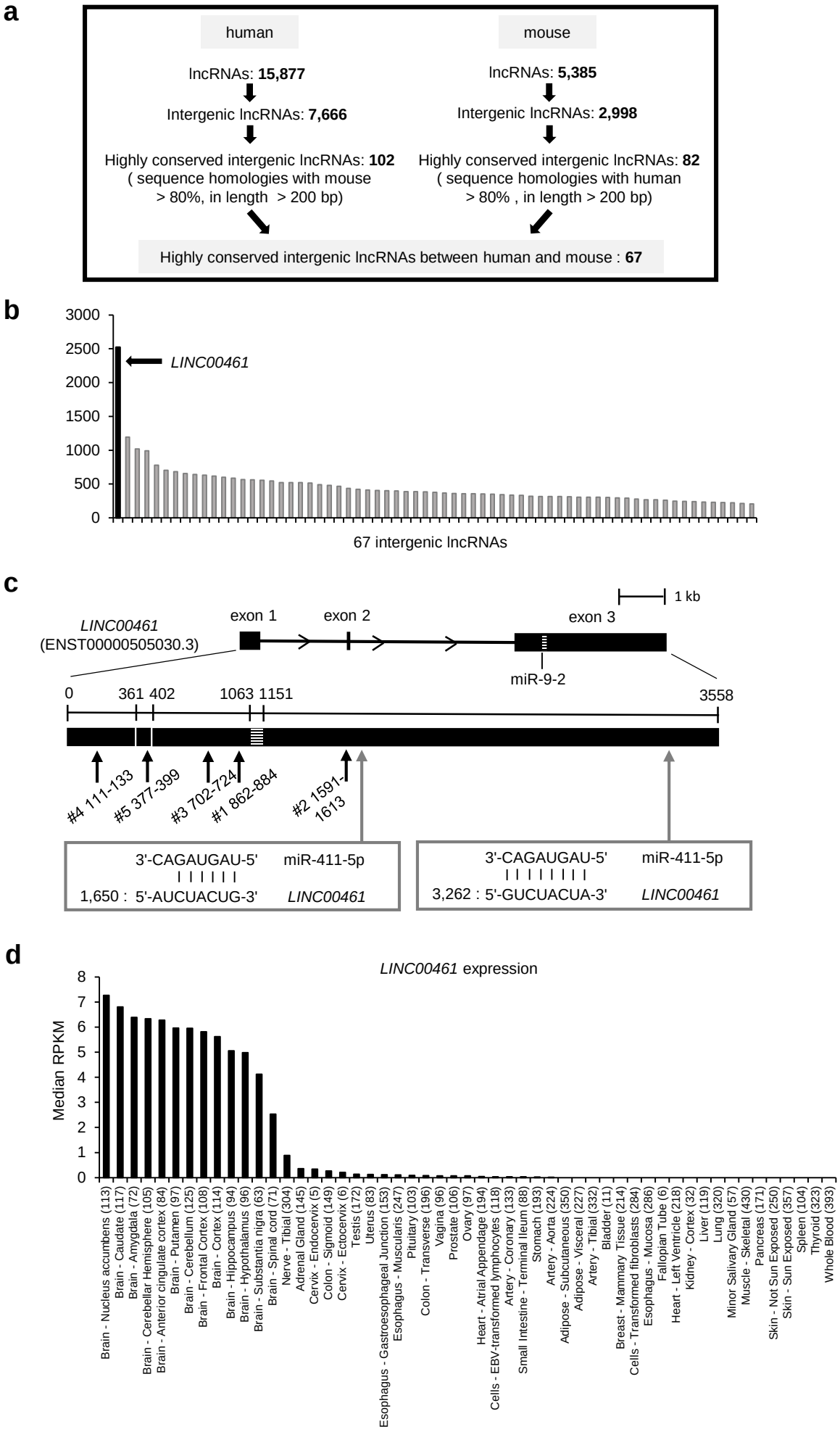
a
human
mouse
lncRNAs: 15,877
Intergenic lncRNAs: 7,666
Highly conserved intergenic lncRNAs: 102
(sequence homologies with mouse
> 80%, in length > 200 bp)
lncRNAs: 5,385
Intergenic lncRNAs: 2,998
Highly conserved intergenic lncRNAs: 82
(sequence homologies with human
> 80% , in length > 200 bp)
Highly conserved intergenic lncRNAs between human and mouse : 67
b
LINC00461
67 intergenic lncRNAs
c
1 kb
LINC00461
(ENST00000505030.3)
exon 1
exon 2
exon 3
miR-9-2
0
361 402
1063 1151
3558
#4 111-133
#5 377-399
#3 702-724
#1 862-884
#2 1591-1613
3'-CAGAUGAU-5'
miR-411-5p
1,650 : 5'-AUCUACUG-3'
LINC00461
3'-CAGAUGAU-5'
miR-411-5p
3,262 : 5'-GUCUACUA-3'
LINC00461
d
LINC00461 expression
Median RPKM
Brain - Nucleus accumbens (113)
Brain - Caudate (117)
Brain - Amygdala (72)
Brain - Cerebellar Hemisphere (105)
Brain - Anterior cingulate cortex (84)
Brain - Putamen (97)
Brain - Cerebellum (125)
Brain - Frontal Cortex (108)
Brain - Cortex (114)
Brain - Hippocampus (94)
Brain - Hypothalamus (96)
Brain - Substantia nigra (63)
Brain - Spinal cord (71)
Nerve - Tibial (304)
Adrenal Gland (145)
Cervix - Endocervix (5)
Colon - Sigmoid (149)
Cervix - Ectocervix (6)
Testis (172)
Uterus (83)
Esophagus - Gastroesophageal Junction (153)
Esophagus - Muscularis (247)
Pituitary (103)
Colon - Transverse (196)
Vagina (96)
Prostate (106)
Ovary (97)
Heart - Atrial Appendage (194)
Cells - EBV-transformed lymphocytes (118)
Artery - Coronary (133)
Small Intestine - Terminal Ileum (88)
Stomach (193)
Artery - Aorta (224)
Adipose - Subcutaneous (350)
Adipose - Visceral (227)
Artery - Tibial (332)
Bladder (11)
Breast - Mammary Tissue (214)
Cells - Transformed fibroblasts (284)
Esophagus - Mucosa (286)
Fallopian Tube (6)
Heart - Left Ventricle (218)
Kidney - Cortex (32)
Liver (119)
Lung (320)
Minor Salivary Gland (57)
Muscle - Skeletal (430)
Pancreas (171)
Skin - Not Sun Exposed (250)
Skin - Sun Exposed (357)
Spleen (104)
Thyroid (323)
Whole Blood (393)

Figure 2

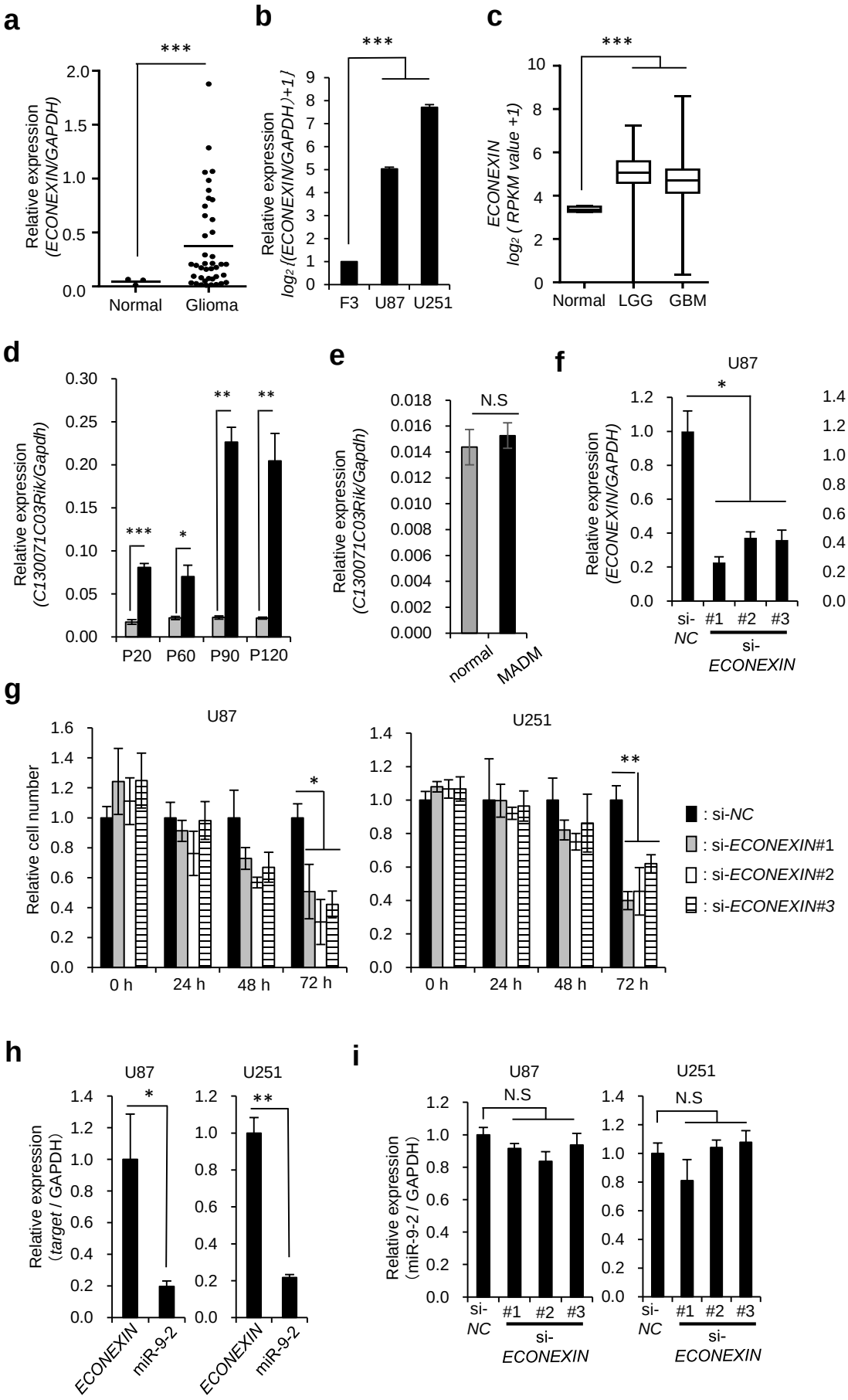
a
b
c
Relative expression (ECONEXIN/GAPDH)
Normal
Glioma
Relative expression log2 /(ECONEXIN/GAPDH)+1/
F3
U87
U251
ECONEXIN log2 (RPKM value +1)
Normal
LGG
GBM
d
Relative expression (C130071C03Rik/Gapdh)
P20
P60
P90
P120
e
N.S
normal
MADM
f
U87
U251
Relative expression (ECONEXIN/GAPDH)
si-NC
#1
#2
#3
si-ECONEXIN
g
U87
U251
Relative cell number
0 h
24 h
48 h
72 h
: si-NC
: si-ECONEXIN#1
: si-ECONEXIN#2
: si-ECONEXIN#3
h
U87
U251
Relative expression (target / GAPDH)
ECONEXIN
miR-9-2
i
U87
U251
N.S
Relative expression (miR-9-2 / GAPDH)
si-NC
#1
#2
#3
si-ECONEXIN

Figure 3

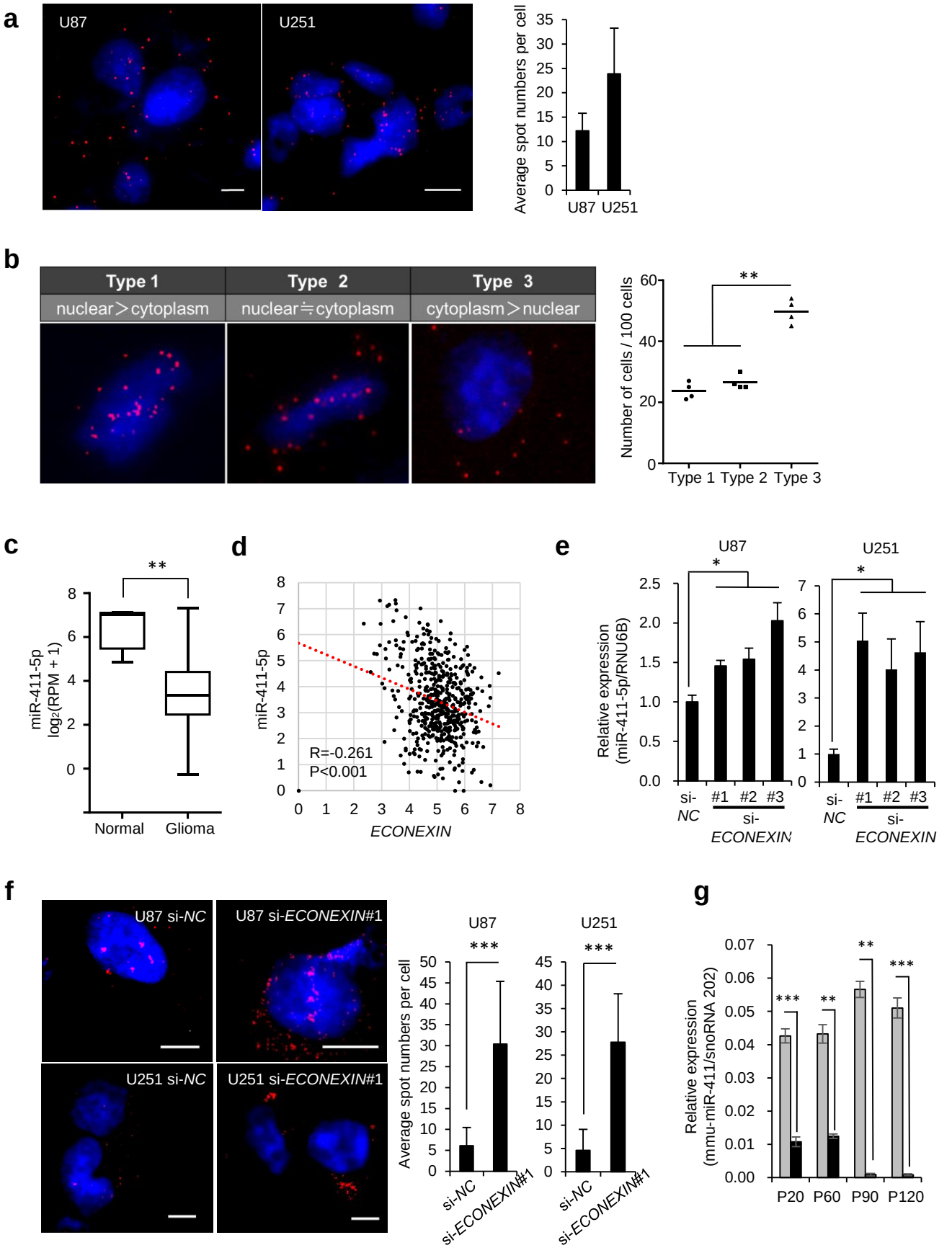
a
U87
U251
Average spot numbers per cell
U87 U251
b
Type 1
nuclear＞cytoplasm
Type 2
nuclear≒cytoplasm
Type 3
cytoplasm＞nuclear
Number of cells / 100 cells
Type 1 Type 2 Type 3
c
miR-411-5p
log2(RPM + 1)
Normal
Glioma
d
miR-411-5p
R=-0.261
P<0.001
ECONEXIN
e
U87
U251
Relative expression
(miR-411-5p/RNU6B)
si-NC
si-ECONEXIN
f
U87 si-NC
U87 si-ECONEXIN#1
U251 si-NC
U251 si-ECONEXIN#1
Average spot numbers per cell
si-NC
si-ECONEXIN#1
g
Relative expression
(mmu-miR-411/snoRNA 202)
P20 P60 P90 P120

Figure 4

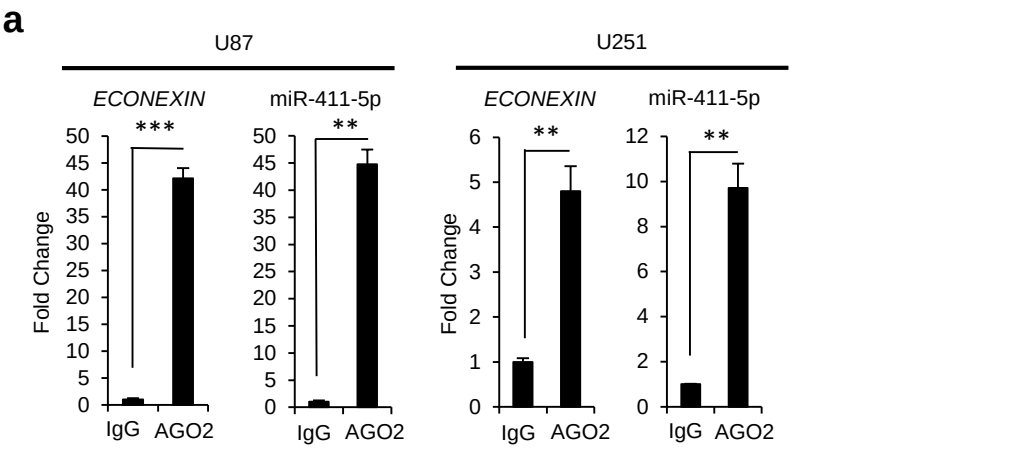
a
U87
U251
ECONEXIN
miR-411-5p
ECONEXIN
miR-411-5p
***
**
**
**
Fold Change
Fold Change
IgG
AGO2
IgG
AGO2
IgG
AGO2
IgG
AGO2

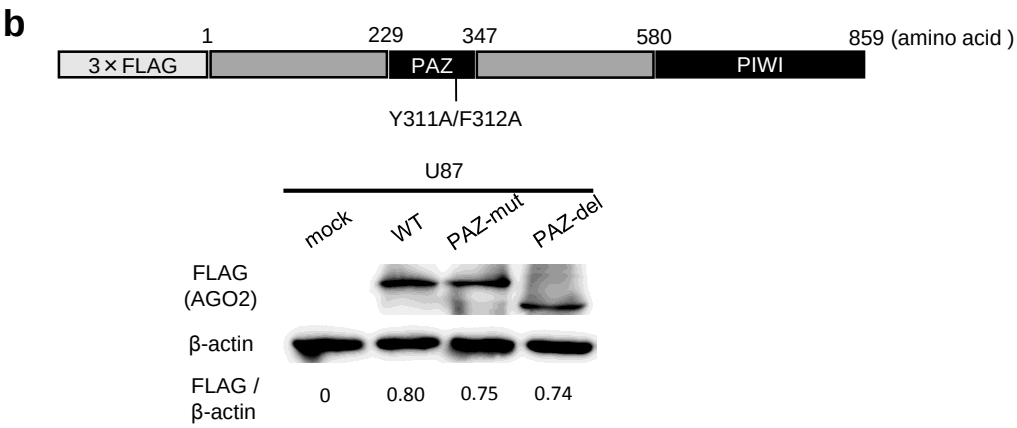
b
1
229
347
580
859 (amino acid)
3×FLAG
PAZ
PIWI
Y311A/F312A
U87
mock
WT
PAZ-mut
PAZ-del
FLAG
(AGO2)
β-actin
FLAG /
β-actin
0
0.80
0.75
0.74

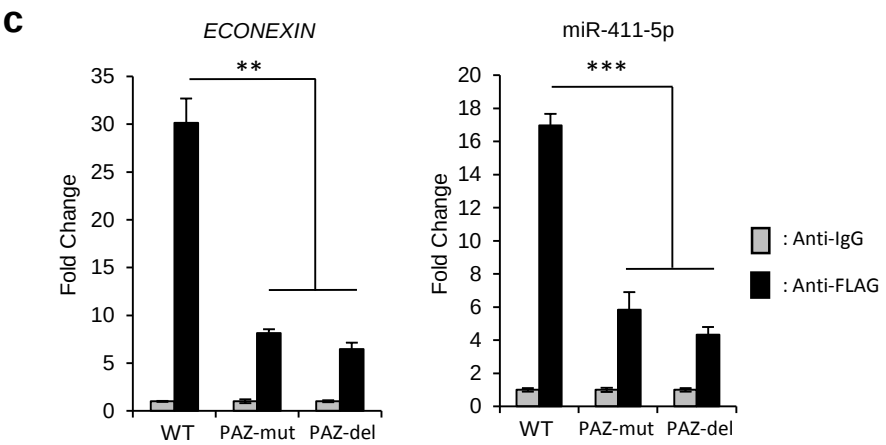
c
ECONEXIN
miR-411-5p
**
***
Fold Change
Fold Change
WT
PAZ-mut
PAZ-del
WT
PAZ-mut
PAZ-del
: Anti-IgG
: Anti-FLAG

Figure 5

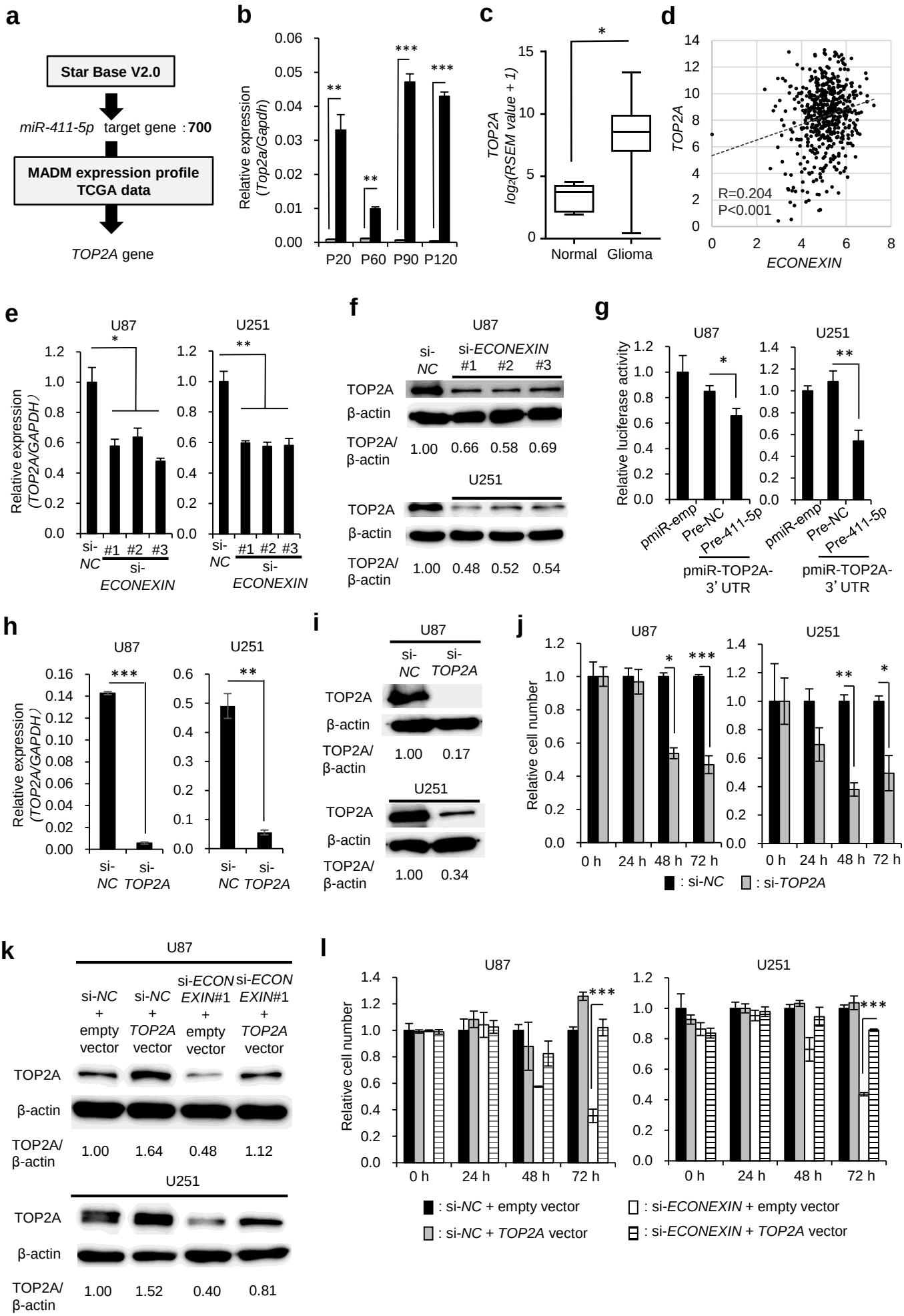
a
Star Base V2.0
miR-411-5p target gene : 700
MADM expression profile TCGA data
TOP2A gene
b
Relative expression (Top2a/Gapdh)
P20 P60 P90 P120
c
TOP2A log2(RSEM value + 1)
Normal Glioma
d
TOP2A
ECONEXIN
R=0.204
P<0.001
e
U87
U251
Relative expression (TOP2A/GAPDH)
si-NC
si-ECONEXIN #1 #2 #3
f
U87
si-NC
si-ECONEXIN #1 #2 #3
TOP2A
β-actin
TOP2A/ β-actin
1.00 0.66 0.58 0.69
U251
1.00 0.48 0.52 0.54
g
U87
U251
Relative luciferase activity
pmiR-emp
Pre-NC
Pre-411-5p
pmiR-TOP2A-3' UTR
h
U87
U251
Relative expression (TOP2A/GAPDH)
si-NC
si-TOP2A
i
U87
si-NC
si-TOP2A
TOP2A
β-actin
TOP2A/ β-actin
1.00 0.17
U251
1.00 0.34
j
U87
U251
Relative cell number
0 h 24 h 48 h 72 h
: si-NC
: si-TOP2A
k
U87
si-NC + empty vector
si-NC + TOP2A vector
si-ECONEXIN#1 + empty vector
si-ECONEXIN#1 + TOP2A vector
TOP2A
β-actin
TOP2A/ β-actin
1.00 1.64 0.48 1.12
U251
1.00 1.52 0.40 0.81
l
U87
U251
Relative cell number
0 h 24 h 48 h 72 h
: si-NC + empty vector
: si-NC + TOP2A vector
: si-ECONEXIN + empty vector
: si-ECONEXIN + TOP2A vector

Supplementary Figure 1

a

species	conservation
Gorilla	○
Old world monkey	○
Cat	○
Cow	○
Sheep	○
Chicken	○
Frog	—
Zebrafish	—
Honey bee	—

b

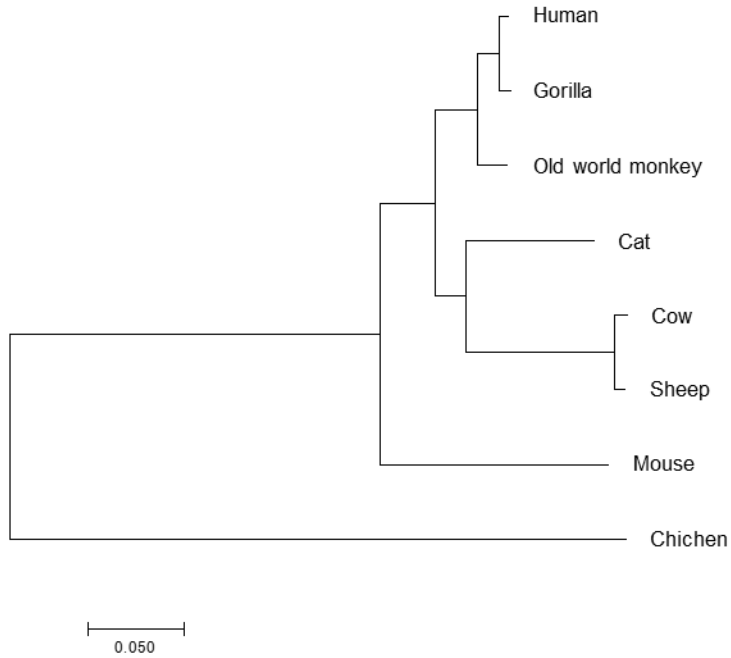

Supplementary Figure 2

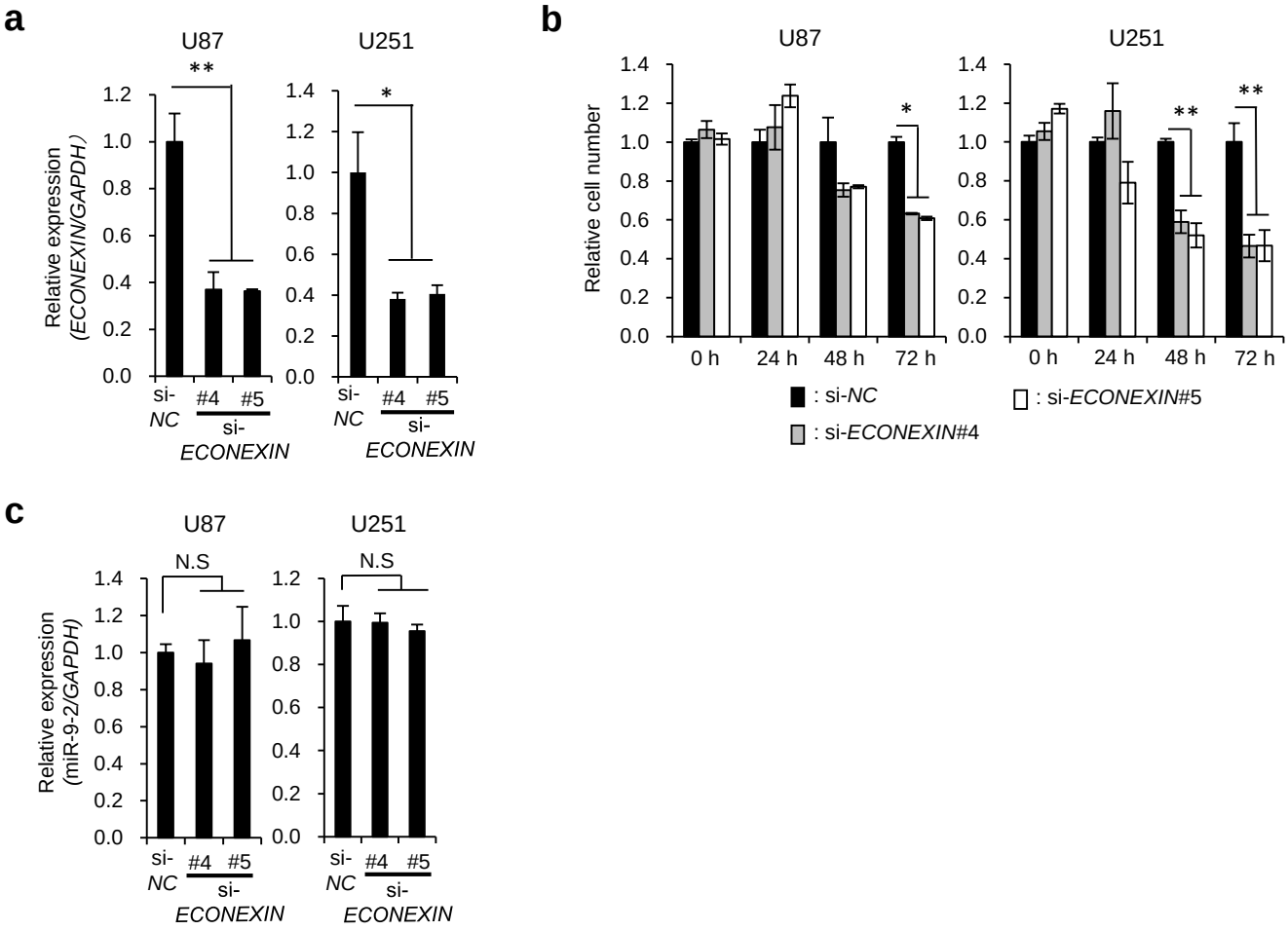

Supplementary Figure 3

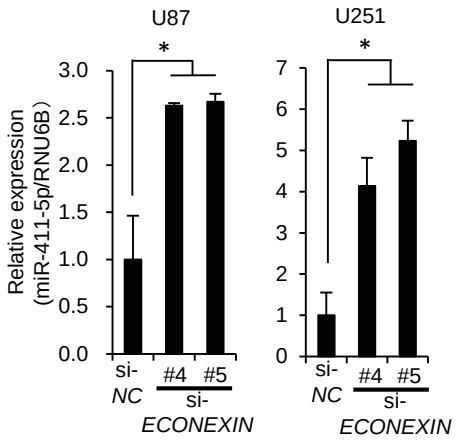

Supplementary Figure 4

a

		3'-gcaugcgauaugcCAGAUGAU-5'	hsa-miR-411-5p
3'UTR	474 :	5'-ucuaguacagauaCUCUACUA-3'	*TOP2A*
		3'-gcaugcgauaugcCAGAUGAU-5'	hsa-miR-411-5p
3'UTR	373 :	5'-cucuuccuccuuUUCUACUU-3'	*TOP2A*
		3'-gcaugcgauacguCAGAUGAU-5'	mmu-miR-411
	3183 :	5'-accuagaaccauuGUCUACUA-3'	*C130071C03Rik*
		3'-gcaugcgauaugcCAGAUGAU-5'	mmu-miR-411
3'UTR	589 :	5'-cguagaguacugaCUCUACUC-3'	*Top2a*

b

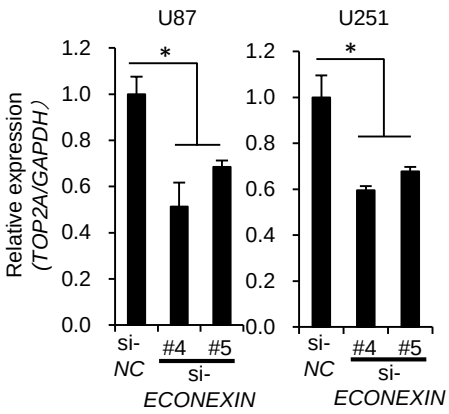

c

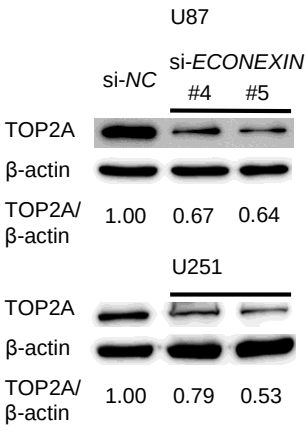

Supplementary Figure legends

Supplementary Figure 1. Characteristics of *ECONEXIN.* (a) Sequence conservation of *LINC00461* between humans and 9 other species. White circle indicates sequence homology >80% in a length >200 bp within the *ECONEXIN* homologues. (b) Phylogenetic tree of *ECONEXIN* homologues from each species. Scale bar represents evolutionary distance (0.05 indicates 5 substitutions per 100 bps).

Supplementary Figure 2. Inhibition of *ECONEXIN* (si-*ECONEXIN* #4.5) decreases glioma cell proliferation. (a) Expression levels of *ECONEXIN* in U87 (left) and U251 cells (right) treated with si-negative control (si-NC), si-*ECONEXIN* #4, or #5. Y-axis indicates expression level relative to si-NC. Experiments were performed in triplicate. Error bars indicate S.D. *, $P<0.05$, **, $P<0.01$. (b) Effects of si-*ECONEXIN #4 and #5* on cell proliferation of U87 (left) and U251 cells (right). X-axis indicates time after transfection of si-RNA. Y-axis indicates cell number relative to si-*NC.* Experiments were performed in triplicate. Error bars indicate S.D. *, $P<0.05$, **, $P<0.01$. (c) Expression level of *miR-9-2* in U87 (left) and U251 cells (right) treated with si-*NC,* si-*ECONEXIN* #4 or #5*.* Y-axis indicates expression level relative to *si-NC*. Experiments were performed in triplicate. Error bars indicate S.D. N.S, not significant

Supplementary Figure 3. Inhibition of *ECONEXIN* (si-*ECONEXIN* #4.5) increases miR-411-5p expression. Expression levels of miR-411-5p in U87 (left) and U251 cells (right) treated with si-*NC,* si-*ECONEXIN* #4 or #5. Y-axis indicates expression level relative to siRNA-negative control (si-*NC*). Experiments were performed in triplicate. Error bars indicate

S.D. *, *P*<0.05.

Supplementary Figure 4. Inhibition of *ECONEXIN* (si-*ECONEXIN* #4.5) decreases TOP2A expression. (a) Upper panels indicates predicted binding sites of miR-411-5p in *Top2a*. Lower panels indicates predicted binding sites of mmu-miR-411 in *C130071C03Rik* and *Top2a*. (b) Expression levels of *TOP2A* in U87 and U251 cells treated with si-*NC,* si-*ECONEXIN #4* or #5. Y-axis indicates expression level relative to siRNA-negative control (si-*NC*). Experiments were performed in triplicate. Error bars indicate S.D. *, *P*<0.05. (c) Protein expression levels of *TOP2A* in U87 and U251 cells treated with si-*NC,* si-*ECONEXIN* #4 or #5.

Supplementary Table 1. Highly conserved intergenic lncRNAs between humans and mice

Gene Name	Transcript ID	Length of Conserved region (bp)	Sequence homology (%)
LINC00461	ENST00000505030.3	2521	82.98
LINC01142	ENST00000440404.5	1193	82.48
RP11-458K10.2	ENST00000470532.1	1019	91.17
MALAT1	ENST00000534336.1	993	81.97
AC004158.2	ENST00000561611.2	779	93.32
MIR137HG	ENST00000424528.2	704	87.5
CTC-529L17.2	ENST00000503489.1	683	84.33
LINC00925	ENST00000536780.4	655	85.5
RP11-681H18.2	ENST00000612252.1	642	83.64
MIR503HG	ENST00000440570.3	633	80.25
LINC00643	ENST00000334389.5	617	89.79
CTD-2249K22.1	ENST00000512859.1	601	98.5
MEG3	ENST00000455531.1	588	83.16
LINC00371	ENST00000563710.3	567	81.83
AC007383.3	ENST00000420509.1	562	87.19
AC007392.3	ENST00000435389.3	556	87.41
RP11-345F18.1	ENST00000504250.1	545	82.94
RP3-418C23.2	ENST00000574739.1	523	88.15
RP11-347I19.7	ENST00000613093.1	522	91.38
AC096649.3	ENST00000438963.1	520	91.73
RP11-340E6.1	ENST00000474979.3	516	83.72
RP11-545H22.1	ENST00000512628.1	489	80.37
RP11-107I14.5	ENST00000450669.2	482	85.27
RP11-204E9.1	ENST00000447728.1	466	85.41
AC093901.1	ENST00000449075.1	437	96.8
RP1-30E17.2	ENST00000449485.1	423	83.22
RP4-665J23.2	ENST00000425185.1	411	90.02
LINC00890	ENST00000569275.1	405	88.89
RP11-308N19.3	ENST00000446206.1	400	80.5
LINC00867	ENST00000445161.3	399	81.45
RP11-684B21.1	ENST00000560056.1	389	85.09
RP11-397G17.1	ENST00000415106.1	388	84.54

RP11-76I14.1	ENST00000545549.1	385	80.26
LINC01109	ENST00000603837.1	379	92.88
RP4-665J23.1	ENST00000606660.1	368	83.97
LINC01412	ENST00000413525.1	360	81.67
AC103564.7	ENST00000437330.1	358	83.8
MEG9	ENST00000429368.1	356	87.08
LINC01505	ENST00000444985.4	353	96.6
RP11-2L8.1	ENST00000450500.1	351	83.48
FLJ37035	ENST00000527483.3	342	83.92
RP1-104O17.1	ENST00000433637.1	337	88.13
RP11-507B12.1	ENST00000559590.1	333	87.69
RP11-159D12.2	ENST00000577267.1	320	80.94
KANTR	ENST00000605526.3	316	84.49
LINC01355	ENST00000566551.1	316	80.06
LINC00599	ENST00000521863.1	314	80.25
RP11-472K22.2	ENST00000512268.1	311	88.42
AC073094.4	ENST00000453798.1	305	95.41
RP11-343J18.2	ENST00000441473.1	305	87.21
RP11-60A8.2	ENST00000511174.1	305	81.64
RP11-271F18.1	ENST00000455871.1	301	87.04
CTD-2012K14.6	ENST00000605277.1	294	82.99
RP11-1008C21.2	ENST00000559232.1	293	89.08
RP11-802H3.2	ENST00000515263.1	279	89.61
RP4-535B20.1	ENST00000448344.1	268	83.96
RP11-107I14.2	ENST00000442188.1	267	80.52
RP4-738P15.1	ENST00000438287.3	261	80.08
LINC01315	ENST00000412060.1	246	85.37
OTX2-AS1	ENST00000534909.2	242	88.43
RP11-290M5.4	ENST00000609367.1	241	95.44
LINC00354	ENST00000412119.1	233	84.12
TUNAR	ENST00000554321.1	230	84.78
MIAT	ENST00000620145.2	227	87.22
RP11-266O8.1	ENST00000556519.2	222	84.68
C1orf132	ENST00000608023.3	212	90.57
RP11-4B14.3	ENST00000482559.1	205	93.17

Supplementary Table 2. Backgrounds of glioma patients

	Grade II	Grade III	Grade IV
Sample number	12	4	24
Mean age (years old)	45.5	44.3	53.9
Male (%)	75	50	79.2
Female (%)	25	50	20.8

Age (years old)	Gender	WHO grade
82	M	IV
82	M	IV
78	F	IV
78	M	IV
77	M	IV
76	M	IV
67	M	IV
67	F	IV
66	F	IV
65	M	IV
59	M	IV
58	M	IV
57	M	IV
56	M	IV
47	M	IV
42	M	IV
40	M	IV
36	M	IV
36	M	IV
35	M	IV
29	M	IV
28	F	IV
23	F	IV
10	M	IV
59	M	III
55	F	III
33	M	III

30	F	III
73	M	II
58	M	II
52	M	II
50	M	II
50	M	II
48	F	II
44	M	II
39	F	II
37	F	II
35	M	II
31	M	II
29	M	II

Supplementary Table 3. Expressions of 700 predicted miR-411-5p target genes in MADM tumors (n=3) and normal mouse brains (n=2)

Gene name	Average of gene expression in MADM (log_2)	Average of gene expression in normal (log_2)	Expression ratio (MADM/normal) (log_2)
TOP2A	11.19493767	4.1605284	7.034409267
CKAP2	9.344965	2.8856164	6.4593486
PBK	10.9954075	5.077962	5.9174455
CDCA5	10.35888067	4.471646	5.887234667
CDK1	7.818162667	2.605294	5.212868667
KIF4A	9.299170167	4.447746	4.851424167
OASL	13.14041717	8.305103	4.835314167
TUBB6	12.48201433	8.08913975	4.392874583
CASC5	6.6426148	2.3809836	4.2616312
C6orf145	6.4358621	2.2560105	4.1798516
PXDC1	6.4358621	2.2560105	4.1798516
VCAN	11.70413	7.58733375	4.11679625
TFPI	11.254461	7.33970015	3.91476085
CENPK	10.30970867	6.5436695	3.766039167
MAP3K1	14.08929433	10.3624095	3.726884833
SOX4	13.07506633	9.5672005	3.507865833
MTBP	11.89828167	8.4142215	3.484060167
TFPI2	5.558894067	2.08898845	3.469905617
FAM111A	9.251714333	5.937359	3.314355333
SCML2	9.261733333	6.01137805	3.250355283
SAMD9	11.32274	8.083223	3.239517
PCDHB2	9.536795667	6.4009826	3.135813067
PRKD3	12.46737933	9.3891455	3.078233833
TRAF3IP2	7.713111767	4.68371125	3.029400517
DRAM1	7.7684438	4.74601475	3.02242905
TUBB2B	16.07383433	13.0775175	2.996316833
IER3	11.78588517	8.815164	2.970721167
ISOC1	12.00272967	9.05297	2.949759667
RAD51	9.228243667	6.3357129	2.892530767
CASP8	10.62461833	7.7509513	2.873667033
ICAM1	7.427212233	4.5645805	2.862631733
LGALS3	11.42582633	8.58668625	2.839140083
RCC2	12.795094	9.9560645	2.8390295
RFC3	9.916803667	7.079398	2.837405667
SRPX	7.7978711	4.967217	2.8306541
ZNF184	10.622722	7.87212895	2.75059305
POU4F1	11.172652	8.44396525	2.72868675
SOX11	11.44767867	8.719468	2.728210667
SHMT1	8.1071195	5.44972785	2.65739165
ADAM12	7.595619833	4.94505685	2.650562983
AIF1L	12.90668267	10.2563715	2.650311167
TNPO1	12.04867533	9.5331385	2.515536833

ACTL6A	11.72275033	9.2198525	2.502897833
SKAP2	12.618853	10.1325055	2.4863475
HERC5	7.992234333	5.57534775	2.416886583
PALLD	10.92391	8.5547745	2.3691355
TMTC2	12.34435233	9.975565	2.368787333
LRRC17	4.6272435	2.2704331	2.3568104
LPP	9.409155667	7.11366615	2.295489517
PAWR	8.440575333	6.174366	2.266209333
C13orf27	10.52838633	8.3199965	2.208389833
HMGN4	13.92341267	11.715461	2.207951667
DDX21	10.7735605	8.5841425	2.189418
MLF1IP	7.723280867	5.58360195	2.139678917
MTHFD2	9.92036	7.8007365	2.1196235
PUS7	12.468984	10.3599125	2.1090715
PPP4R1	14.09485683	11.99153	2.103326833
ZNF146	11.66878233	9.5711815	2.097600833
POLD1	11.732299	9.645311	2.086988
CYBRD1	8.0838369	6.0056215	2.0782154
SS18	14.11558233	12.055675	2.059907333
ZNF655	10.53922733	8.561806	1.977421333
NHSL1	12.12592733	10.1576835	1.968243833
HCLS1	11.635642	9.6890325	1.9466095
CROT	12.26801367	10.3379355	1.930078167
ARHGAP18	9.548047	7.63547885	1.91256815
EYA1	15.0297465	13.170573	1.8591735
LARS	13.30717633	11.4789	1.828276333
GPR56	13.33601267	11.5106575	1.825355167
SP1	11.764234	9.964281	1.799953
ARL6IP6	13.8575035	12.0607835	1.79672
ZNF800	8.382414667	6.5957147	1.786699967
DTL	9.110019667	7.3479525	1.762067167
C1orf144	10.52352733	8.7695215	1.754005833
PDE3B	10.28752833	8.536499	1.751029333
SLC7A6	8.604131333	6.87858535	1.725545983
ROD1	9.059855	7.351861	1.707994
MTHFD1L	11.36663167	9.659465	1.707166667
C16orf80	13.760375	12.0605075	1.6998675
POLR2D	11.38461833	9.687041	1.697577333
NRF1	9.831534667	8.134284	1.697250667
PRMT6	9.042447	7.3694912	1.6729558
CNPY4	9.252001333	7.58660075	1.665400583
KPNA2	13.416049	11.7560565	1.6599925
HMMR	10.95662267	9.303328	1.653294667
TOR1AIP2	10.320505	8.6839075	1.6365975
EPB41L5	7.324287633	5.7122538	1.612033833
BTBD7	6.569314733	4.957443	1.611871733

C14orf147	11.97519133	10.363698	1.611493333
ERH	15.31675367	13.7531035	1.563650167
PPIE	8.922634667	7.3673362	1.555298467
CCNK	13.71288933	12.1877805	1.525108833
TANC1	9.361559	7.83677435	1.52478465
TRAM1	10.178868	8.667819	1.511049
CNIH4	13.61134067	12.10617125	1.505169417
C9orf30	11.69050233	10.18583275	1.504669583
FAT4	8.117183667	6.61786185	1.499321817
STK17A	10.04415033	8.544891	1.499259333
MDC1	10.20663467	8.70921025	1.497424417
SSRP1	13.78975633	12.2978595	1.491896833
MOBKL1B	9.813573	8.3239795	1.4895935
RUVBL2	13.402765	11.9161415	1.4866235
MPHOSPH6	11.9304925	10.445779	1.4847135
XRN2	12.78236333	11.3082875	1.474075833
GKAP1	12.33944767	10.868156	1.471291667
FAM129A	6.3482872	4.89919115	1.44909605
BZW1	12.2464565	10.8003185	1.446138
YEATS2	12.24813167	10.80285325	1.445278417
NFIA	8.832175	7.4225929	1.4095821
RPL7	16.59612733	15.190894	1.405233333
MAML3	8.972285667	7.58088885	1.391396817
HSD17B4	14.098134	12.711978	1.386156
C15orf23	11.457782	10.073535	1.384247
PFN1	11.57100767	10.227104	1.343903667
FANCD2	6.727573233	5.3840162	1.343557033
ANKRD57	10.13229683	8.79559475	1.336702083
C7orf27	11.53980117	10.2073715	1.332429667
ITFG3	13.01707233	11.685719	1.331353333
ZNF516	6.010824	4.680294	1.33053
SMAD4	12.62974233	11.306637	1.323105333
MDFIC	10.25332067	8.930839	1.322481667
GATM	12.507838	11.1986085	1.3092295
C11orf54	12.40355433	11.0994685	1.304085833
TOR1AIP1	10.152193	8.8500565	1.3021365
FAM46A	10.29806633	9.006315	1.291751333
TNS3	12.24492367	10.9554515	1.289472167
IL20RB	5.918272467	4.63060985	1.287662617
ARID2	9.260570333	7.97375385	1.286816483
HNRPA1	12.49367133	11.217175	1.276496333
HNRPA1L-2	12.49367133	11.217175	1.276496333
HNRNPA1	12.49367133	11.217175	1.276496333
NAB1	10.47960367	9.2184305	1.261173167
JMJD1C	12.16534533	10.905525	1.259820333
PRKCQ	9.156520667	7.896846	1.259674667

FARSA	11.591929	10.3353415	1.2565875
PATZ1	9.303815	8.0473167	1.2564983
MAGED1	15.83678567	14.5935955	1.243190167
HNRPA3	14.06221033	12.819583	1.242627333
HNRNPA3	14.06221033	12.819583	1.242627333
FAM108B1	12.80785733	11.577971	1.229886333
UTP11L	12.36110333	11.1336195	1.227483833
PCBP2	13.97468233	12.7480655	1.226616833
SLC4A7	10.98394833	9.7583305	1.225617833
PAIP1	9.949900333	8.72644425	1.223456083
HLTF	10.84015133	9.6199445	1.220206833
SET	12.90068233	11.6825095	1.218172833
PSMB2	10.88040367	9.66334	1.217063667
TXNIP	10.465087	9.2499435	1.2151435
PTPN13	10.42627133	9.219359	1.206912333
TSLP	4.487806133	3.2888168	1.198989333
HIF1A	9.789705	8.59326575	1.19643925
MAPRE1	11.82648433	10.6361505	1.190333833
TARBP2	13.3119	12.1260405	1.1858595
PRRC1	8.978159	7.7954525	1.1827065
EML4	11.80067767	10.6278295	1.172848167
HEY2	7.1979391	6.0284076	1.1695315
PTPN12	10.35982767	9.191547	1.168280667
RNF182	11.46697467	10.306935	1.160039667
EEF1A1	16.455541	15.299085	1.156456
RBMX	11.59832933	10.442985	1.155344333
NUP54	10.97761233	9.824371	1.153241333
ETAA1	8.324199	7.176437	1.147762
FERMT2	11.84417417	10.7014495	1.142724667
SLC22A5	8.831096667	7.7022585	1.128838167
DOLPP1	13.31661	12.1878165	1.1287935
KTI12	11.06163367	9.9361385	1.125495167
SP2	9.432627667	8.3084485	1.124179167
GOLPH3	12.601464	11.4785995	1.1228645
CYTH4	11.39768133	10.2845995	1.113081833
FKBP7	9.6844	8.5756295	1.1087705
ZNF280C	11.04141967	9.935876	1.105543667
ANUBL1	6.159305167	5.07758015	1.081725017
DNAJB12	10.56126067	9.484518	1.076742667
SF3B3	13.567712	12.49131725	1.07639475
FRZB	9.991494	8.915726	1.075768
RAB10	13.266819	12.1959405	1.0708785
ITSN2	12.05704567	11.00214275	1.054902917
ZNF518A	7.377331533	6.3250036	1.052327933
ZNF518	7.377331533	6.3250036	1.052327933
EDARADD	4.029586433	2.98139425	1.048192183

EIF2A	10.504455	9.467629	1.036826
PPAT	9.009667667	7.974397	1.035270667
API5	11.23180317	10.1974675	1.034335667
PSAT1	13.535467	12.503781	1.031686
SCFD1	10.52893633	9.5022405	1.026695833
C22orf28	13.28180533	12.256732	1.025073333
DBT	7.401514033	6.3791883	1.022325733
SGPP1	14.22805633	13.206455	1.021601333
MTA1	10.64938933	9.628594	1.020795333
C21orf91	10.47373733	9.4544045	1.019332833
FAM96A	12.62596083	11.606862	1.019098833
TMOD3	8.232307467	7.21521425	1.017093217
PSMD11	11.950075	10.9395845	1.0104905
E2F3	10.20489267	9.195873	1.009019667
ZKSCAN3	10.72101167	9.715803	1.005208667
ASCC3	10.66187817	9.657851	1.004027167
RBM26	11.71016867	10.71008925	1.000079417
NIPBL	8.80799	7.817832	0.990158
TOPORS	11.20194867	10.21494075	0.987007917
ZNRF2	8.0146098	7.03955555	0.97505425
PDCL	9.953663667	8.9791635	0.974500167
TAF4	11.65959267	10.69551	0.964082667
HDGF	13.021522	12.06166125	0.95986075
EIF2C1	8.480873333	7.52236635	0.958506983
TRPS1	11.03014067	10.0731595	0.956981167
EXOSC3	8.996855333	8.041357	0.955498333
SFXN2	10.47972333	9.5244285	0.955294833
HNRPUL1	10.33144333	9.376985	0.954458333
HNRNPUL1	10.33144333	9.376985	0.954458333
MAP3K7	10.927119	9.9788975	0.9482215
HADH	11.320406	10.3847225	0.9356835
RPL28	16.40758667	15.473649	0.933937667
RAB9A	13.146196	12.21427	0.931926
DHX15	11.24813967	10.333324	0.914815667
TMCO6	8.537101333	7.635406	0.901695333
SAMD4B	12.511014	11.612382	0.898632
FAM160A1	8.784096	7.8888055	0.8952905
SNRPD1	13.50794467	12.622444	0.885500667
BRD2	13.577374	12.695143	0.882231
ZNF281	13.253466	12.37727	0.876196
LRBA	10.57858	9.7101795	0.8684005
UBE2R2	13.38001767	12.5171495	0.862868167
C2orf74	3.003217	2.14190945	0.86130755
PTPRG	9.115675167	8.2599755	0.855699667
SYF2	11.42494467	10.570776	0.854168667
CTDSPL2	7.9055282	7.05172515	0.85380305

MITD1	9.495519	8.6424985	0.8530205
SEC63	9.605885333	8.7542955	0.851589833
ZNF10	13.12742017	12.27662325	0.850796917
MTM1	7.646483267	6.7971245	0.849358767
MEX3C	12.4137885	11.564801	0.8489875
HMGN3	12.71123983	11.8637745	0.847465333
UBE2E3	13.31413333	12.4708635	0.843269833
PDCD2	11.56265167	10.71992025	0.842731417
SASS6	8.587290333	7.7454782	0.841812133
SLC7A5	11.47384367	10.6320525	0.841791167
TIGD2	10.252726	9.413437	0.839289
COG2	9.213897167	8.3839445	0.829952667
PM20D2	6.2989598	5.4720385	0.8269213
C9orf64	7.863701	7.0368717	0.8268293
ALDH3B1	9.785112667	8.960691	0.824421667
XPO7	9.806207	8.982202	0.824005
RPS27A	16.51564067	15.6918965	0.823744167
ZBTB34	6.866484667	6.0450654	0.821419267
NKAP	9.195523	8.3774275	0.8180955
CLIP2	11.17279	10.358368	0.814422
ARPC1A	14.03846533	13.225184	0.813281333
PRDM4	10.30967417	9.4969665	0.812707667
DNAJC19	11.25638767	10.452262	0.804125667
CCDC47	11.73332633	10.931982	0.801344333
PSMA2	15.80439733	15.0058565	0.798540833
KIAA1191	13.95924067	13.1628085	0.796432167
PSMA3	15.27619883	14.4929255	0.783273333
ARL6IP1	13.96232183	13.180584	0.781737833
PRPF38B	10.00931167	9.231162	0.778149667
EIF1AX	13.02006967	12.242232	0.777837667
ZNF384	6.867789133	6.09267865	0.775110483
FAM165B	13.50808867	12.743062	0.765026667
SCARB2	10.730769	9.9688165	0.7619525
TMEM39A	9.660569	8.9073545	0.7532145
NAA15	10.76999883	10.0172195	0.752779333
CTDP1	9.901161333	9.149449	0.751712333
NT5C3L	10.71542233	9.967143	0.748279333
PPP2R3A	6.577442433	5.8327077	0.744734733
MPP6	13.205576	12.464245	0.741331
FAM122B	8.427989	7.6878641	0.7401249
C1orf131	11.4241785	10.686046	0.7381325
CEP76	8.061292733	7.3278961	0.733396633
STAT6	7.748803433	7.0196965	0.729106933
EGLN3	7.628265967	6.9009892	0.727276767
ZC3H11A	14.04229733	13.320265	0.722032333
ZSCAN12	10.79773167	10.07598	0.721751667

RPL9	17.49996133	16.7800435	0.719917833
PTGES3	13.58813767	12.868388	0.719749667
DDX3X	13.4936	12.7766475	0.7169525
PAK1IP1	13.55931267	12.846343	0.712969667
TNRC6B	9.689875667	8.97833925	0.711536417
LRRC59	11.301553	10.5995015	0.7020515
C14orf119	10.55518967	9.8543315	0.700858167
RIT1	13.76958933	13.0743055	0.695283833
SPOPL	8.043102567	7.355728	0.687374567
BCL7B	11.21988367	10.541217	0.678666667
TMCO1	12.101512	11.429836	0.671676
KIF2A	9.452399667	8.7856165	0.666783167
HNRNPH1	14.99481933	14.333635	0.661184333
HNRPH1	14.99481933	14.333635	0.661184333
CTSA	13.48982233	12.8311805	0.658641833
PDS5A	9.215477	8.5579885	0.6574885
DIAPH2	10.62390567	9.968658	0.655247667
RPL26L1	15.97318867	15.3189	0.654288667
PPP1R12A	12.65975433	12.00622	0.653534333
SFRS11	11.41057	10.7610435	0.6495265
NUTF2	12.705992	12.0666155	0.6393765
SRP19	11.77192333	11.139446	0.632477333
TMEM188	10.92748033	10.3007225	0.626757833
STXBP3	11.095598	10.471581	0.624017
ZEB2	10.45435433	9.8319135	0.622440833
CSNK1E	11.921135	11.3055505	0.6155845
RPL4	15.17975333	14.5648335	0.614919833
PPP6C	12.068744	11.4559705	0.6127735
CNBP	13.740117	13.127783	0.612334
C2orf29	8.991943	8.380669	0.611274
ANKRD17	11.94080067	11.33413025	0.606670417
MED21	11.14159367	10.548392	0.593201667
BRD4	13.26419367	12.6734365	0.590757167
ZNF85	6.616636167	6.03524835	0.581387817
FOXO1	11.52472133	10.94465	0.580071333
FOXO1A	11.52472133	10.94465	0.580071333
ACVR1	11.71697633	11.1440155	0.572960833
ZBTB26	7.686974833	7.11812515	0.568849683
RSBN1	9.851864167	9.286532	0.565332167
BIRC6	10.42141217	9.8563525	0.565059667
KTN1	12.740367	12.17646075	0.56390625
PATL1	9.262394	8.6999805	0.5624135
CLIC4	11.73545867	11.1733885	0.562070167
HOXA10	4.213144967	3.6510829	0.562062067
YOD1	8.493824667	7.93247735	0.561347317
GTF2IP1	14.04781	13.48916	0.55865

KIAA1143	9.462226333	8.9077655	0.554460833
ANKRA2	13.1203675	12.5664645	0.553903
ELL	12.04305167	11.489632	0.553419667
CPT1A	10.34946733	9.799435	0.550032333
FAM192A	11.731589	11.181962	0.549627
ARAP2	10.307713	9.7593975	0.5483155
TIPRL	10.63746367	10.0901355	0.547328167
EPB41L2	8.794291	8.2556725	0.5386185
RNF149	11.36055	10.82867675	0.53187325
POLR2A	9.275875667	8.7444035	0.531472167
MAGEF1	10.689974	10.1612265	0.5287475
UBE2L3	14.027295	13.49873825	0.52855675
ARIH2	12.87555567	12.357152	0.518403667
WBP5	12.37341233	11.862783	0.510629333
MYH9	12.37811167	11.8702955	0.507816167
HEATR2	9.681272	9.1768095	0.5044625
MRPL44	11.581505	11.077092	0.504413
PPP1CC	14.36415633	13.86223975	0.501916583
RAB21	9.58748	9.0875005	0.4999795
FAM114A2	12.04244267	11.54326625	0.499176417
RSRC2	11.07299433	10.576798	0.496196333
HMBOX1	8.984691667	8.4887855	0.495906167
EED	12.03852767	11.5468795	0.491648167
SDCCAG1	12.326123	11.8351515	0.4909715
SAPS3	8.968611667	8.4829725	0.485639167
FUT8	10.951779	10.46860025	0.48317875
LRRC57	10.88937867	10.411121	0.478257667
CHUK	12.459115	11.985941	0.473174
PIGO	12.59320267	12.122987	0.470215667
CDH2	13.499508	13.0366405	0.4628675
APPL1	11.06090467	10.59809425	0.462810417
CDKN2AIP	6.941651367	6.4800188	0.461632567
ACTG1	16.52307067	16.063874	0.459196667
GOLT1B	11.15495717	10.696702	0.458255167
MRPL42	11.448289	10.9911155	0.4571735
RAD23B	10.38233433	9.930453	0.451881333
TMEM38B	6.0282082	5.58102485	0.44718335
ZNF711	10.02747117	9.581473	0.445998167
MRPL35	9.478753667	9.054354	0.424399667
UBA6	8.172925	7.7488902	0.4240348
C7orf60	9.043251333	8.621266	0.421985333
CAMLG	12.597606	12.1803	0.417306
PUM1	12.368029	11.9532115	0.4148175
ZFP36	2.719485367	2.3093946	0.410090767
ABCA11P	8.107929667	7.69810035	0.409829317
RPAP3	12.697974	12.2932355	0.4047385

PLA1A	7.7574976	7.3614845	0.3960131
MLL5	11.3105585	10.921768	0.3887905
CYB5A	14.22998833	13.8450235	0.384964833
NCK2	11.05282133	10.670069	0.382752333
UGT8	11.12815767	10.7491605	0.378997167
ERICH1	6.932701367	6.55526255	0.377438817
GRK5	8.684448667	8.30946025	0.374988417
HSPA4	12.30820733	11.93805	0.370157333
NUFIP2	11.48359333	11.117281	0.366312333
MYLIP	9.188353333	8.8442415	0.344111833
DYRK1A	8.960179333	8.623358	0.336821333
DDX50	10.78899783	10.454258	0.334739833
MYST2	13.49850567	13.166882	0.331623667
RANBP2	11.044413	10.7141715	0.3302415
S100PBP	7.2220536	6.89271305	0.32934055
WSB1	9.295123	8.975541	0.319582
USP34	9.844100333	9.525011	0.319089333
TSEN15	12.36043933	12.0424535	0.317985833
SLC35A5	7.221875333	6.9088235	0.313051833
SERINC3	13.884642	13.5741045	0.3105375
C1orf35	11.55478067	11.25494075	0.299839917
PPFIA1	10.574596	10.276806	0.29779
PIAS2	11.22387867	10.935567	0.288311667
FAM18B	11.04391967	10.75617775	0.287741917
CDC42SE2	12.65318267	12.366041	0.287141667
USP48	11.347884	11.0613715	0.2865125
USP25	9.667973667	9.3952525	0.272721167
LEF1	10.43159533	10.1726055	0.258989833
SDHB	15.04432	14.78738	0.25694
SHPRH	7.768260533	7.5126476	0.255612933
WWP1	8.051860133	7.796494	0.255366133
GOLGA2	13.46896367	13.2198	0.249163667
GLUD1	14.17524667	13.928764	0.246482667
CAMSAP1L1	9.191947	8.9496975	0.2422495
EIF4G2	12.090261	11.849496	0.240765
RALGDS	11.71140433	11.4736995	0.237704833
ZNF235	9.6403365	9.40318575	0.23715075
SMARCD2	8.067492833	7.8362415	0.231251333
NUDT4	13.08851367	12.8599435	0.228570167
NUDT4P1	13.08851367	12.8599435	0.228570167
PKD1	12.09181333	11.8639325	0.227880833
PDK1	9.062059667	8.834268	0.227791667
SRGAP2	9.067219167	8.846632	0.220587167
TMED3	13.751069	13.531832	0.219237
UBE2D1	7.349367533	7.1320193	0.217348233
ALDH3A2	9.626151667	9.410587	0.215564667

CEP55	6.4713698	6.25650735	0.21486245
AP3S1	11.67902167	11.4647465	0.214275167
SAE1	11.49945917	11.2869705	0.212488667
MGAT4A	7.842548667	7.63477725	0.207771417
NUMA1	13.326883	13.1275775	0.1993055
MBNL1	11.57254167	11.374435	0.198106667
DUSP11	8.209455	8.01685075	0.19260425
C1orf55	9.749012	9.557061	0.191951
TM4SF1	11.94979133	11.758792	0.190999333
TRIM33	10.240359	10.049575	0.190784
LRRFIP1	11.39851033	11.2087305	0.189779833
ORC5L	8.5886675	8.400017	0.1886505
VCPIP1	10.872761	10.6877045	0.1850565
NISCH	16.26442067	16.080325	0.184095667
FAM133B	9.537814667	9.3541265	0.183688167
MGC40405	9.537814667	9.3541265	0.183688167
SIRT7	11.289323	11.1100215	0.1793015
ZNF148	11.80478933	11.6286175	0.176171833
TMEM200B	3.686916633	3.5187699	0.168146733
NEDD8	14.5481705	14.383052	0.1651185
C12orf66	10.24941367	10.0895995	0.159814167
GFPT1	10.81721533	10.658652	0.158563333
NRBP1	12.05195233	11.898632	0.153320333
CTSB	15.31927267	15.174771	0.144501667
BPNT1	9.245479667	9.1072435	0.138236167
COL4A1	9.9055725	9.77018	0.1353925
YPEL5	10.94790433	10.814909	0.132995333
FAM160B1	12.09945467	11.9688185	0.130636167
ZRANB3	7.650254233	7.524397	0.125857233
ACSS2	10.900509	10.7799135	0.1205955
CCDC71	11.670102	11.5506715	0.1194305
MID1IP1	14.152342	14.0338035	0.1185385
CACHD1	10.2285685	10.110708	0.1178605
ZNF236	8.936669	8.819343	0.117326
PCDHA1	4.344098333	4.2400979	0.104000433
TNRC6A	10.84121867	10.73869175	0.102526917
SLTM	13.019364	12.9188355	0.1005285
KIF3A	13.036739	12.9386785	0.0980605
PDXDC1	9.922680667	9.8283915	0.094289167
HOXA13	3.446191867	3.3553231	0.090868767
FBXL5	9.474731333	9.384101	0.090630333
AK3	12.935957	12.84621	0.089747
ZDHHC21	10.1356645	10.0481725	0.087492
ATP5F1	13.62961267	13.54302	0.086592667
ACBD5	9.385822333	9.3019115	0.083910833
FAS	7.6992079	7.6153353	0.0838726

C1orf109	9.443861667	9.3616705	0.082191167
TMEM30A	11.48839	11.416312	0.072078
FSTL5	10.74537733	10.676923	0.068454333
ZNF646	6.918685867	6.85081475	0.067871117
MIB1	10.370216	10.315217	0.054999
ARRDC3	8.896145667	8.852864	0.043281667
KIAA0494	11.92758333	11.8850995	0.042483833
CUTC	6.576739633	6.53463415	0.042105483
MYO18A	11.50076033	11.458709	0.042051333
OVOL2	11.60201833	11.560376	0.041642333
CLTB	11.47718267	11.4380395	0.039143167
SVIP	12.33004333	12.294543	0.035500333
HNRPH3	8.540294667	8.5050685	0.035226167
HNRNPH3	8.540294667	8.5050685	0.035226167
NPEPPS	13.04731017	13.013276	0.034034167
UBE2E2	13.78405633	13.7506	0.033456333
TMEM134	11.98169233	11.9577115	0.023980833
C5orf41	6.587165333	6.5670827	0.020082633
CAPZA2	12.58081967	12.5681145	0.012705167
SCML1	2.354425867	2.3459189	0.008506967
TOM1L1	11.40290033	11.397205	0.005695333
IGSF3	9.928223333	9.9265355	0.001687833
PDS5B	9.862373667	9.864843	-0.002469333
TARSL2	11.42246933	11.4374335	-0.014964167
FAM18B2	10.175684	10.1932825	-0.0175985
AXIN2	4.749037467	4.77437115	-0.025333683
AKAP9	11.871409	11.898516	-0.027107
YME1L1	7.494506233	7.5275979	-0.033091667
CIRH1A	11.39184	11.437048	-0.045208
CAT	10.450668	10.49774325	-0.04707525
NCKAP1	14.02692567	14.0856715	-0.058745833
KLHDC5	8.916073333	8.980655	-0.064581667
PRKAR1A	12.55782733	12.62793	-0.070102667
ZCCHC10	9.641000667	9.7123385	-0.071337833
MSL1	13.267942	13.3402475	-0.0723055
MSL-1	13.267942	13.3402475	-0.0723055
ZNRF3	6.616273133	6.6895093	-0.073236167
ZDHHC17	10.94823633	11.021534	-0.073297667
HNRNPH2	11.103904	11.178838	-0.074934
UNKL	5.985900233	6.0617349	-0.075834667
NOG	7.309365267	7.388024	-0.078658733
FNIP1	11.435613	11.516924	-0.081311
ARF1	15.256873	15.348452	-0.091579
RPS6KA5	8.632861	8.724488	-0.091627
C12orf75	9.421273833	9.521531	-0.100257167
CCNE1	10.25640667	10.357795	-0.101388333

C12orf4	10.61039167	10.712795	-0.102403333
CGRRF1	10.03357017	10.1464975	-0.112927333
FAM178A	8.284600767	8.400291	-0.115690233
ZFR	7.754366667	7.877913	-0.123546333
RNF19A	11.309954	11.43887575	-0.12892175
SEMA4D	9.897528	10.0269665	-0.1294385
TMEM170A	8.377891667	8.5106885	-0.132796833
ARHGAP28	7.5880931	7.73192	-0.1438269
PEA15	13.82505933	13.9695115	-0.144452167
STIM2	7.7785526	7.92402695	-0.14547435
ZC3H13	10.93117583	11.0820265	-0.150850667
RNMT	9.851374333	10.005055	-0.153680667
ZFYVE21	10.513293	10.6848225	-0.1715295
FAM49B	10.98356433	11.1580445	-0.174480167
POLK	7.618777467	7.79444365	-0.175666183
CREM	8.3861128	8.5652215	-0.1791087
ZBTB38	8.1358152	8.316282	-0.1804668
SUCLG1	13.54598733	13.7277175	-0.181730167
C3orf52	3.5607469	3.74693125	-0.18618435
UBE2V2	12.05168167	12.24245675	-0.190775083
CELF1	11.88589967	12.0830305	-0.197130833
VLDLR	11.457448	11.6680295	-0.2105815
CREBZF	10.96209533	11.18086	-0.218764667
ZF	10.96209533	11.18086	-0.218764667
IMMT	12.23348067	12.4584715	-0.224990833
FOXG1	13.453163	13.683055	-0.229892
RAPGEF2	12.76868067	12.9994665	-0.230785833
SLMAP	11.175495	11.4097655	-0.2342705
TMEM216	9.951063667	10.1890265	-0.237962833
UBE4A	9.909663333	10.152771	-0.243107667
UBE2N	12.56183	12.8097835	-0.2479535
YAF2	12.67235633	12.921328	-0.248971667
STARD4	8.598857	8.8480245	-0.2491675
C17orf71	1.737531767	1.9913844	-0.253852633
LOC440248	12.34574067	12.600986	-0.255245333
ASAP1	10.78869933	11.0607815	-0.272082167
EXD2	8.536598667	8.820965	-0.284366333
OLA1	12.06643133	12.3514965	-0.285065167
MTMR4	9.218658333	9.5138205	-0.295162167
OCRL	11.979835	12.281157	-0.301322
GADD45A	8.634649667	8.94306	-0.308410333
BBS2	9.061666333	9.389736	-0.328069667
RYBP	12.274737	12.616579	-0.341842
GCNT2	8.376630167	8.727686	-0.351055833
PIGK	8.610945533	8.9654205	-0.354474967
STON2	6.614778367	6.98561925	-0.370840883

ARHGAP5	9.582782667	9.9555475	-0.372764833
TMCC1	9.591185	9.969172	-0.377987
CAMSAP1	10.98071617	11.3673645	-0.386648333
MNX1	2.662742867	3.055465	-0.392722133
CCDC91	10.08490567	10.479166	-0.394260333
NDFIP1	15.28807233	15.694662	-0.406589667
PTPLAD1	15.10839433	15.522724	-0.414329667
CBWD1	8.510827667	8.9279335	-0.417105833
CBWD5	8.510827667	8.9279335	-0.417105833
ENC1	14.926894	15.3475415	-0.4206475
C1S	5.712193367	6.134924	-0.422730633
FBXO33	10.74888917	11.1779835	-0.429094333
NDUFA5	15.01706867	15.44720125	-0.430132583
PLCL2	12.16204167	12.6175765	-0.455534833
SLC16A9	7.278990433	7.7348343	-0.455843867
Kua	7.747335067	8.20966475	-0.462329683
TMEM189	7.747335067	8.20966475	-0.462329683
DUSP1	9.820587667	10.31625725	-0.495669583
MICB	4.564319433	5.06018775	-0.495868317
GHITM	13.70630167	14.20532775	-0.499026083
NUB1	12.21879983	12.724183	-0.505383167
IPO7	7.990636	8.4965035	-0.5058675
AKT3	11.17457367	11.6880635	-0.513489833
SH3BP5	9.865592667	10.3881775	-0.522584833
SC5DL	10.872775	11.3958445	-0.5230695
SH3BGRL2	7.440453333	7.96968735	-0.529234017
PHLPP2	10.40592967	10.936602	-0.530672333
TMEM65	10.14398533	10.6769745	-0.532989167
COL4A5	6.5221753	7.0623648	-0.5401895
KCTD12	9.883777833	10.4408545	-0.557076667
TUSC3	12.74822017	13.310978	-0.562757833
UBFD1	10.58395467	11.1498955	-0.565940833
UBE2W	9.811682333	10.38336225	-0.571679917
EGR1	13.497957	14.070696	-0.572739
USP32	12.56942267	13.15562075	-0.586198083
KLF4	9.185409833	9.7868945	-0.601484667
LRP12	10.20010533	10.803612	-0.603506667
WASF1	13.06895567	13.6733725	-0.604416833
CDC42EP3	9.315261	9.9219165	-0.6066555
APLP2	14.6111025	15.2254535	-0.614351
PIK3R6	10.03912967	10.654058	-0.614928333
CYLD	11.94282233	12.5945085	-0.651686167
FAM129B	11.748755	12.40305375	-0.65429875
GPD2	9.901104667	10.560238	-0.659133333
HDGFRP3	11.55979067	12.223469	-0.663678333
CPEB4	7.532716033	8.2130225	-0.680306467

MYL12B	14.413844	15.110799	-0.696955
TMEM9B	13.27402967	13.97350425	-0.699474583
BCAS4	9.277151	9.9787605	-0.7016095
PFN2	13.82191733	14.524282	-0.702364667
RNF6	13.277984	13.9810505	-0.7030665
PAFAH1B1	13.447666	14.1639415	-0.7162755
TECPR2	9.707360667	10.4391045	-0.731743833
HERPUD1	12.022726	12.7569885	-0.7342625
CLIP1	10.073685	10.821334	-0.747649
CLASP2	6.556482867	7.31822485	-0.761741983
ARFGEF2	8.6401645	9.407491	-0.7673265
KIAA1324L	8.995288667	9.7842435	-0.788954833
PPP1R9A	11.841578	12.647974	-0.806396
GADD45B	9.378380167	10.18825225	-0.809872083
ZMAT2	13.228039	14.0590575	-0.8310185
AUTS2	8.566506333	9.410874	-0.844367667
SLC20A1	12.35033967	13.1975235	-0.847183833
C12orf34	8.927219	9.7759385	-0.8487195
GNAQ	11.39532467	12.2590095	-0.863684833
ACSL1	10.40712633	11.2955485	-0.888422167
RUNX1T1	10.554712	11.4438095	-0.8890975
LYSMD2	11.95001867	12.8611645	-0.911145833
ISCA1	11.681055	12.609982	-0.928927
AKTIP	10.349402	11.2851205	-0.9357185
PFKM	14.15487467	15.0920675	-0.937192833
TLE4	6.7755346	7.71809965	-0.94256505
NEGR1	9.510857333	10.460776	-0.949918667
PPARG	7.9792308	8.9397705	-0.9605397
MBNL2	11.56707767	12.5457645	-0.978686833
BTRC	10.69247	11.686335	-0.993865
PHF15	12.37131833	13.379538	-1.008219667
RNF14	13.5302745	14.5434255	-1.013151
HSP90AA1	13.97251267	14.993994	-1.021481333
PPTC7	12.168459	13.202816	-1.034357
AUH	10.786573	11.8320765	-1.0455035
MEGF8	11.84077733	12.8871425	-1.046365167
ABT1	4.840745833	5.89794635	-1.057200517
AP1B1	13.11195533	14.171299	-1.059343667
GSK3A	13.796452	14.858959	-1.062507
SYBU	9.864202667	10.929427	-1.065224333
TOMM70A	10.557896	11.625362	-1.067466
PROK2	4.6598262	5.75037885	-1.09055265
ELMO2	8.135605467	9.2317065	-1.096101033
MAP7D2	10.28183	11.4207245	-1.1388945
LOC150786	12.982867	14.1792055	-1.1963385
PDLIM1	10.39069333	11.6151195	-1.224426167

MAP2K1	12.48229567	13.716871	-1.234575333
SMARCA2	10.88608133	12.1244865	-1.238405167
CAMKK2	12.8089115	14.050014	-1.2411025
OXR1	11.73885567	12.98967075	-1.250815083
CALM1	15.65122	16.9556255	-1.3044055
REEP5	11.55542567	12.932383	-1.376957333
CELSR1	7.728699167	9.12277475	-1.394075583
CHSY3	5.313862833	6.76258135	-1.448718517
C5orf23	5.850678133	7.33065715	-1.479979017
NPR3	5.850678133	7.33065715	-1.479979017
MMD	11.08337633	12.61058575	-1.527209417
C17orf65	6.231619767	7.78656505	-1.554945283
L1CAM	7.510627167	9.087492	-1.576864833
PNOC	9.160971333	10.7939505	-1.632979167
TTLL11	8.445152	10.096302	-1.65115
LPGAT1	10.82093967	12.48566	-1.664720333
NRXN3	9.930639667	11.6281585	-1.697518833
STMN1	14.56718933	16.322691	-1.755501667
ADRBK1	12.07454767	13.85847575	-1.783928083
CAMK1D	10.025003	11.8451955	-1.8201925
KLC1	11.00575033	12.88402525	-1.878274917
MAP1B	10.19971067	12.1019095	-1.902198833
LPPR4	10.20632333	12.1533535	-1.947030167
SEMA3A	6.706816733	8.6601	-1.953283267
FLRT2	6.986485733	9.0488225	-2.062336767
ROBO2	7.8601465	9.944533	-2.0843865
PAK1	11.47429433	13.561988	-2.087693667
PRR16	2.9898541	5.0982571	-2.108403
MLLT11	13.40149233	15.523164	-2.121671667
NOV	6.94895	9.0730645	-2.1241145
BNIP3	11.63875833	13.7746475	-2.135889167
BMP6	6.297023667	8.510147	-2.213123333
PLCXD2	10.28670133	12.5517845	-2.265083167
KIF21A	11.076628	13.3606855	-2.2840575
DUSP5	3.340393867	5.72126865	-2.380874783
ZNF483	3.473055	5.85734585	-2.38429085
PREPL	9.386301667	11.7787345	-2.392432833
CACNB4	9.237837667	11.6662525	-2.428414833
LEPRE1	9.402561667	11.8599265	-2.457364833
TMEM74	5.024459867	7.50901245	-2.484552583
TRIM37	11.900515	14.4084515	-2.5079365
PRDM8	7.6409638	10.2139255	-2.5729617
ATP1B1	13.65787783	16.3473775	-2.689499667
EFHD1	8.263604633	11.0071155	-2.743510867
FAIM3	2.624274167	5.40133975	-2.777065583
CDS1	7.033244633	9.9707135	-2.937468867

LUM	5.150454233	8.181677	-3.031222767
FGF9	7.915199667	11.4172335	-3.502033833
MAL2	9.020901433	13.3227485	-4.301847067
C9orf41	N/A	N/A	N/A
ZNF721	N/A	N/A	N/A
ZNF200	N/A	N/A	N/A
LOC645323	N/A	N/A	N/A
ZNF567	N/A	N/A	N/A
ZNF680	N/A	N/A	N/A
LRRC37B2	N/A	N/A	N/A
ZNF197	N/A	N/A	N/A
LOC100093631	N/A	N/A	N/A
LOC100132987	N/A	N/A	N/A
GIMAP2	N/A	N/A	N/A

N/A : not applicable

Supplementary Table 4. Expressions of 13 transcriptional factors in MADM model mice and Glioma tissues

MADM mouse model

	MADM / Normal (log_2)	MADM (log_2)	Normal (log_2)	P value
SOX3	6.330985	14.33052	7.999534	0.000794
PRRX1	2.641517	9.561797	6.92028	0.000789
TCF3	2.141706	10.86213	8.720428	0.002462
SOX9	1.940535	11.54724	9.606703	0.037565
TCF12	1.89209	10.46643	8.574336	0.004121
SP1	1.799953	11.76423	9.964281	0.003437
NRF1	1.697251	9.831535	8.134284	0.000173
SP3	1.622128	3.558814	1.936686	0.001093
ATF1	1.317528	9.347354	8.029826	5.33E-05
HLTF	1.220207	10.84015	9.619945	0.012216
ELK4	1.047303	8.270951	7.223648	0.010908
HINFP	0.910814	8.081337	7.170523	0.047654
TCF4	0.848959	13.63375	12.78479	0.021845

Glioma tissues

	Glioma / Normal (log_2)	Glioma (log_2)	Normal (log_2)	P value
TCF12	2.876284	12.89876	10.02248	0.001095
SOX3	2.785636	6.879216	4.09358	0.001797
PRRX1	2.749149	10.63573	7.88658	0.000677
TCF3	1.933415	10.82735	8.89394	0.000538
SP1	0.969601	10.38584	9.41624	0.027065
SOX9	0.938038	11.8588	10.92076	2.73E-05
TCF4	0.665662	12.31098	11.64532	5.26E-06
SP3	0.625978	10.47168	9.8457	0.001198
ATF1	0.552589	7.696289	7.1437	0.005152
HLTF	0.392144	10.336	9.94386	0.010001
ELK4	0.353717	6.127337	5.77362	0.034357
NRF1	0.327728	8.775868	8.44814	0.018198
HINFP	0.189566	8.805186	8.61562	0.000622

Supplementary Table 5. Primer sequences in this study

Oligonucleotide primers used for TaqMan PCR assays

Target gene	AB assay ID
GAPDH	Hs00266705_g1
hsa-miR-9-2	Hs03303202_pri
miR-411	001610
RNU6B	001093
snoRNA202	001232

Primer sequences for SYBR green PCR assays

Target gene	Primer sequence (5' to 3')
LINC00461	Forward: GACAATCCAACCAACCAAAGA Reverse: TAGGGGGAAGATCCTCGATT
TOP2A	Forward: CAAACAAAGGGACCCAAAAA Reverse: CAACTTTGTGTTCAACAACAGGA
C130071C03Rik (mouse)	Forward: TGACACTTCAAAGAAGCATAAAATG Reverse: TGTGAATGTTTTAAGGGAGATCCT
Top2a (mouse)	Forward: GCCATCTTCTTCTGATAGCTCTG Reverse: TATCGTGTCTTCCAAGTCCACA
Gapdh (mouse)	Forward: GAATTTGCCGTGAGTGGAGT Reverse: CGTCCCGTAGACAAAATGGT

Supplementary Table 6. siRNA targeting sequences for each gene

Target gene	Targeted sequence (5' to 3')
LINC00461 #1	AAGAAAAGTTCGGAATAAACTCT
LINC00461 #2	GTCAATTTGTACGAAATTAGACT
LINC00461 #3	GAGAAAGAAGCAATTTACAATGC
LINC00461 #4	ACCCATTTAAACTATTTTAGACG
LINC00461 #5	AGCATAAAATGAATAGACAATCC
TOP2A (Santa Cruz Biotechnology)	Catalog No.sc-36695

Supplementary Table 7. Primer sequences for construction of FLAG-AGO2 variant vector

Target gene	Primer sequence (5' to 3')
AGO2 with mutated PAZ domain (Y311A/F312A)	Forward: GCAGCTCAAGGACAGGCACA Reverse: TGGGCCACCGTGCACTC
AGO2 with deleted PAZ domain	Forward: CTGTGCCTTGTAAAACGCT Reverse: GCAGGACAAAGATGTATTAAAAAA

Supplementary Table 8. Primer sequences for manipulation of *TOP2A* analyses

Primer sequences for manipulation of *TOP2A* 3'-UTR pmir-GLO luciferase reporter vector

Gene	Primer sequence (5' to 3')
TOP2A-3'UTR	Forward: GCCTCGAGAATGTGAGGCGATTATTTTAAGTAA Reverse: ACTCTAGATTCTATGGGTTGCAATGTTTAGAAC

Primer sequences for manipulation of *TOP2A* vector with gateway cloning technology

Gene	Primer sequence (5' to 3')
TOP2A	Forward: CACCATGGAAGTGTCACCATTGCA Reverse: TTAAAACAGATCATCTTCATCTGACTC